Models in spintronics (Part I)

OUTLINE :

Spin-dependent transport in metallic magnetic multilayers

-Introduction to spin-electronics

-Spin-dependent scattering in magnetic metal

-Current-in-plane Giant Magnetoresistance

-Modelling transport in CIP spin-valves

-Current-perpendicular-to-plane Giant Magnetoresistance

-Spin accumulation, spin current, 3D generalization.

Birth of spin electronics : Giant magnetoresistance (1988)

Fe/Cr multilayers

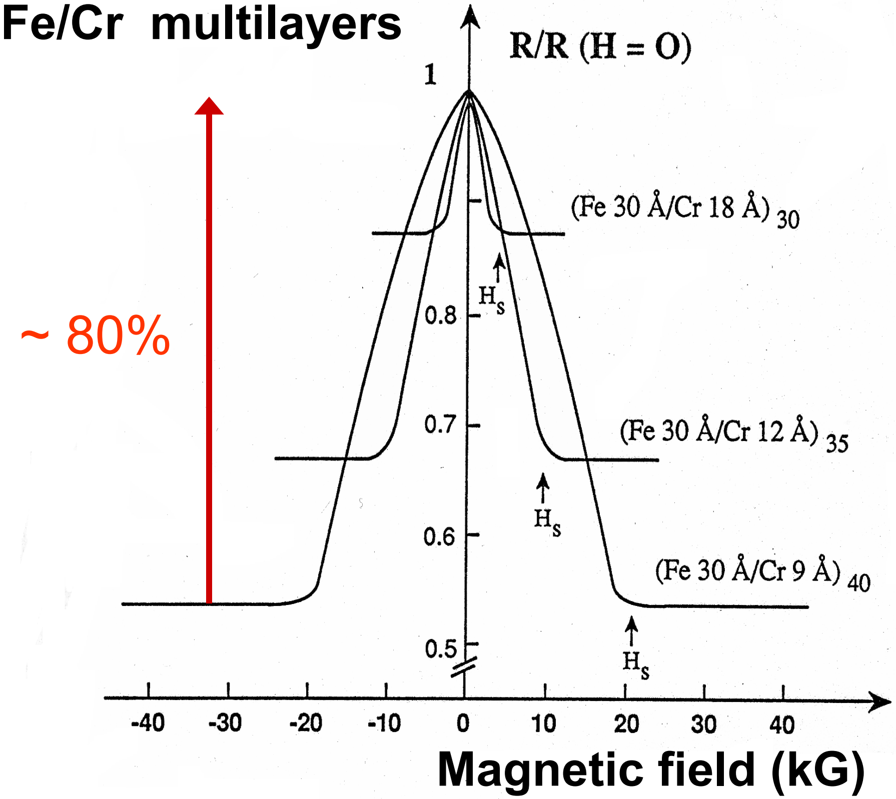

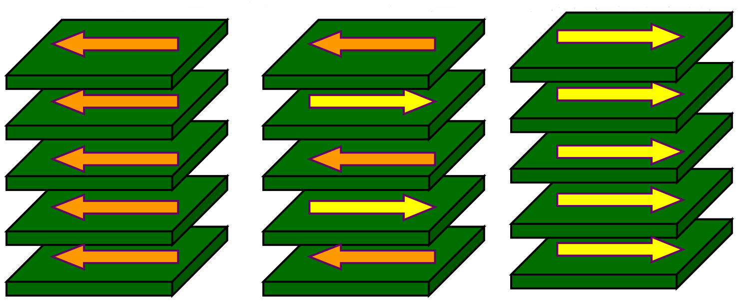

Antiferromagnetically coupled multilayers

Fert et al, PRL (1988), Nobel Prize 2007

Two limit geometries of measurement:

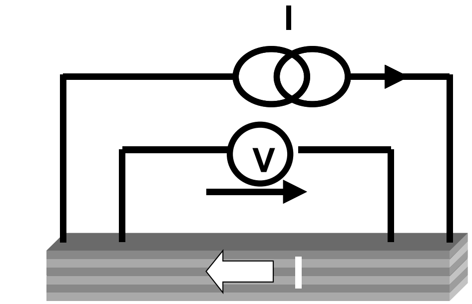

Current-in-plane

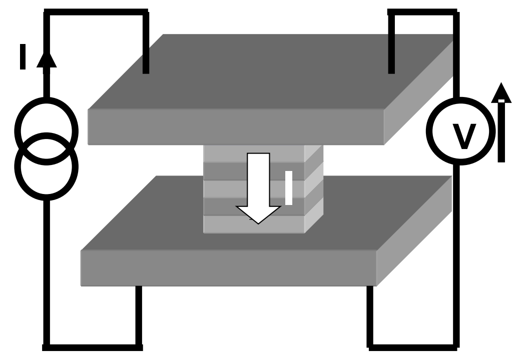

Current-perpendicular-to-plane

$$GMR = \frac{R_{AP} - R_P}{R_P}$$

Low field GMR: Spin-valves

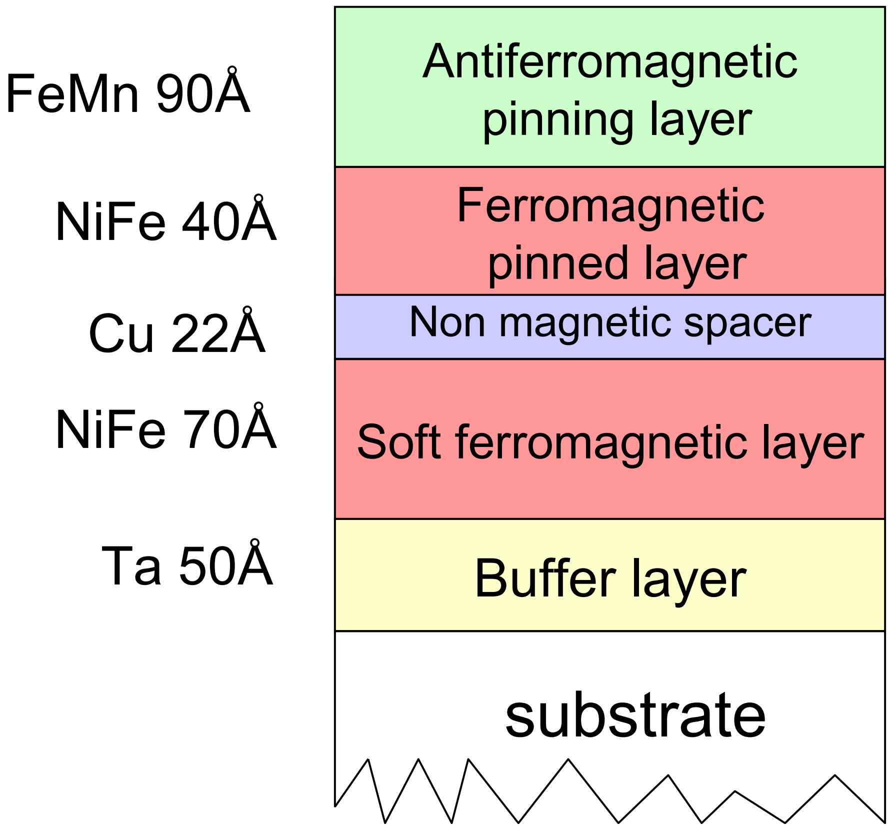

IBM Almaden

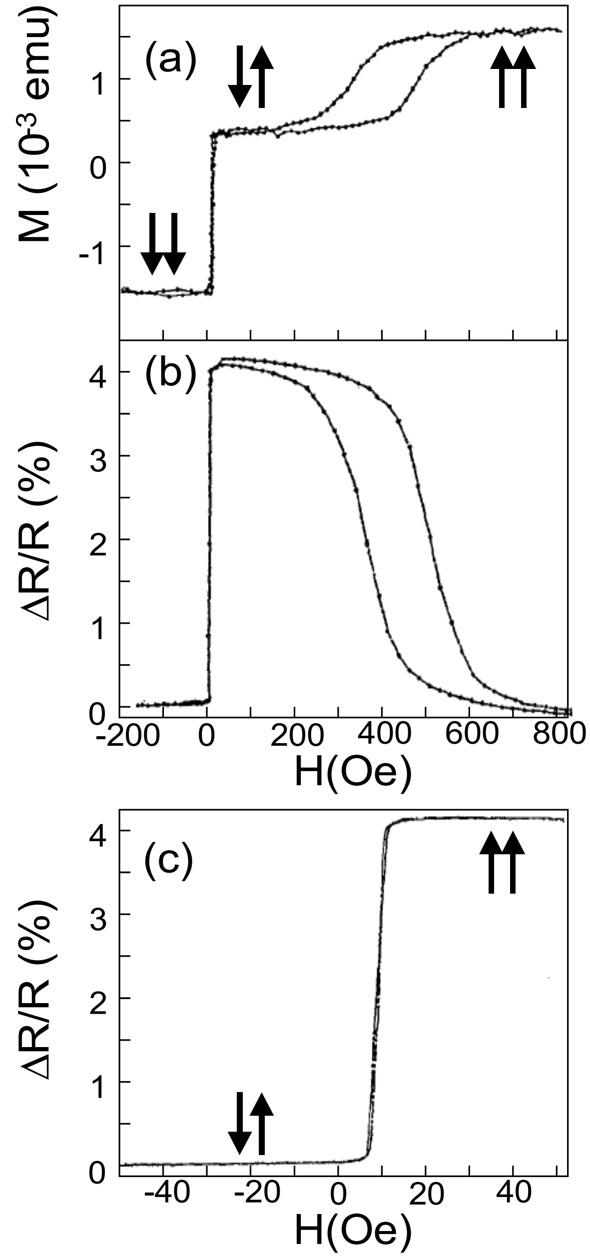

Ultrasensitive magnetic field sensors (MR heads)
Spin engineering

B.Dieny et al, Phys.Rev.B.(1991)+patent US5206590 (1991).

Benefit of GMR in magnetic recording

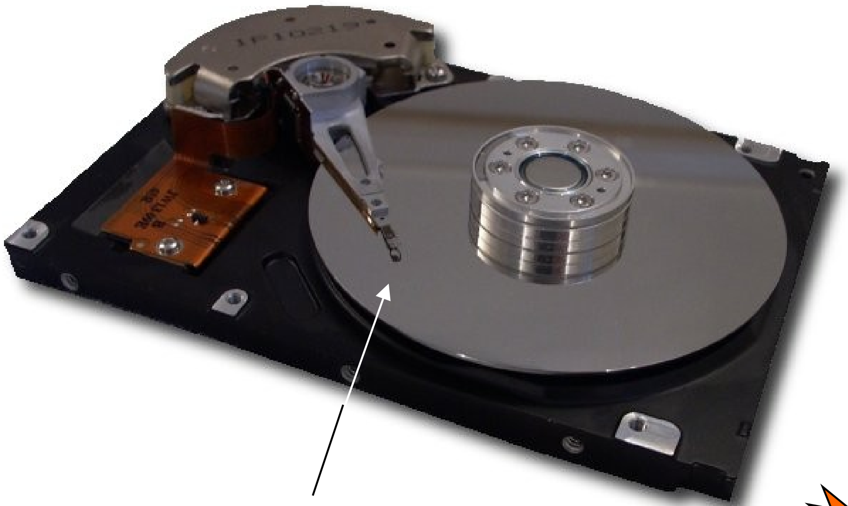

GMR spin-valve heads from 1998 to 2004

Two current model (Mott 1930) for transport in magnetic metals

As long as spin-flip is negligible, current can be considered as carried in parallel by two categories of electrons: spin ↑ and spin ↓ (parallel and antiparallel to quantization axis)

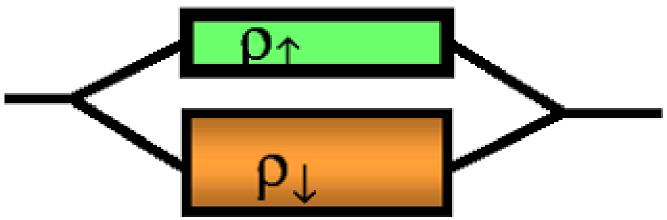

$$\rho = \left(\frac{1}{\rho_\uparrow} + \frac{1}{\rho_\downarrow} \right)^{-1} = \frac{\rho_\uparrow \rho_\downarrow}{\rho_\uparrow + \rho_\downarrow}$$

Sources of spin flip: magnons and spin-orbit scattering

Negligible spin-flip often crude approximation (spin diffusion length in NiFe~4.5nm, 30% spin memory loss at Co/Cu interfaces)

Band structure of 3d transition metals

In transition metals, partially filled bands which participate to conduction are s and d bands

Non-magnetic Cu :

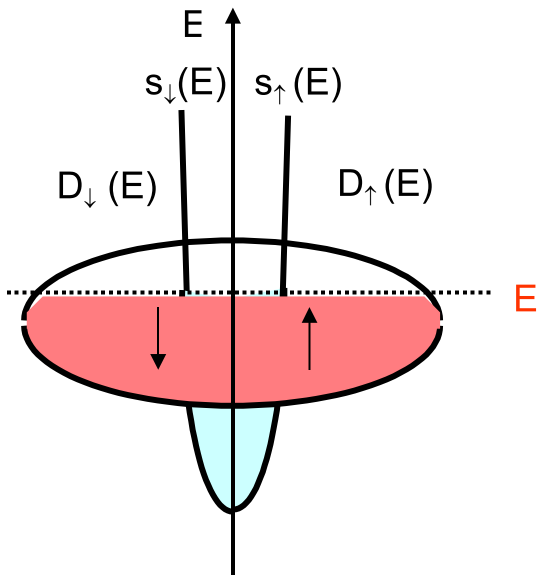

$D_\uparrow(E_F) = D_\downarrow(E_F)$

Magnetic Ni :

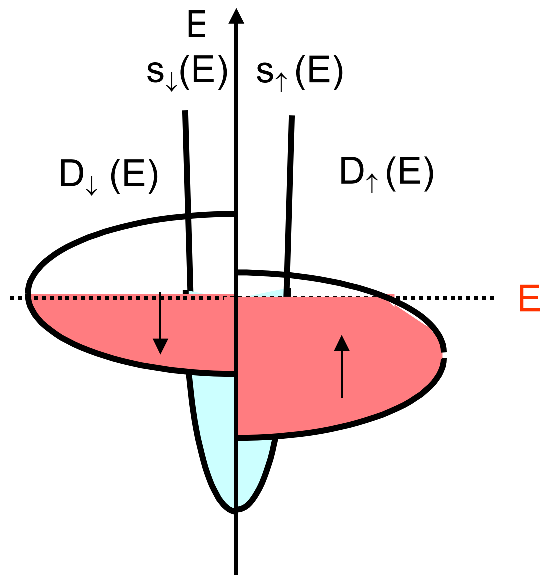

$D_\uparrow(E_F) \neq D_\downarrow(E_F)$

Most of transport properties are determined by DOS at Fermi energy

$\boxed{\text{Spin-dependent density of state at Fermi energy}}$

$m^*(d) \gg m^*(s)$ ⇒ J mostly carried by s electrons in transition metals

Scattering of electrons determined by DOS at E_F :

Fermi Golden rule : $P^\sigma \propto \langle i|W|f\rangle^2 D_f(E_F)$

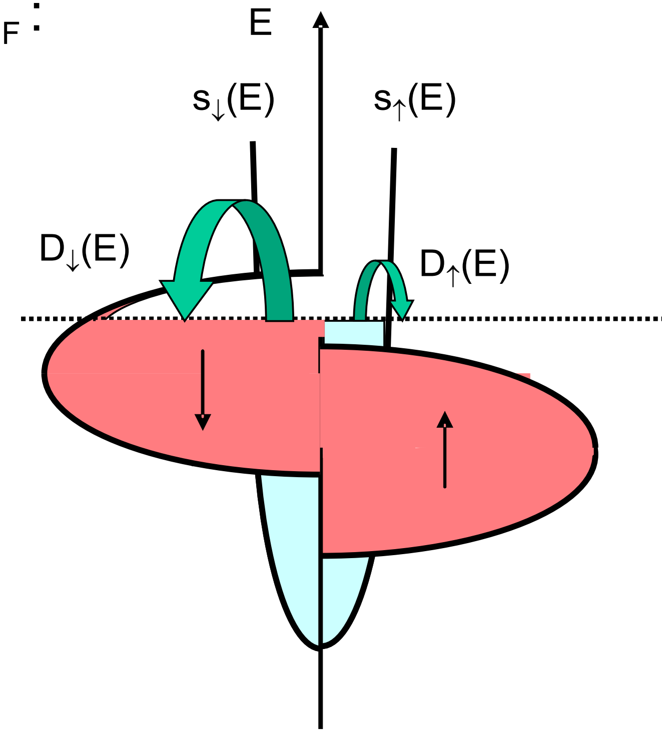

$s_\uparrow \rightarrow s_\uparrow$

$s_\uparrow \rightarrow d_\uparrow$

$s_\downarrow \rightarrow s_\downarrow$

$s_\downarrow \rightarrow d_\downarrow$ Most efficient scattering channel

⇒ Spin-dependent scattering rates in magnetic transition metals

Example: $\lambda_{\uparrow Co} = 10nm; \lambda_{\downarrow Co} = 1nm$

Potential experienced by conduction electrons in magnetic metallic multilayers

Parallel magnetic configuration

Antiparallel magnetic configuration

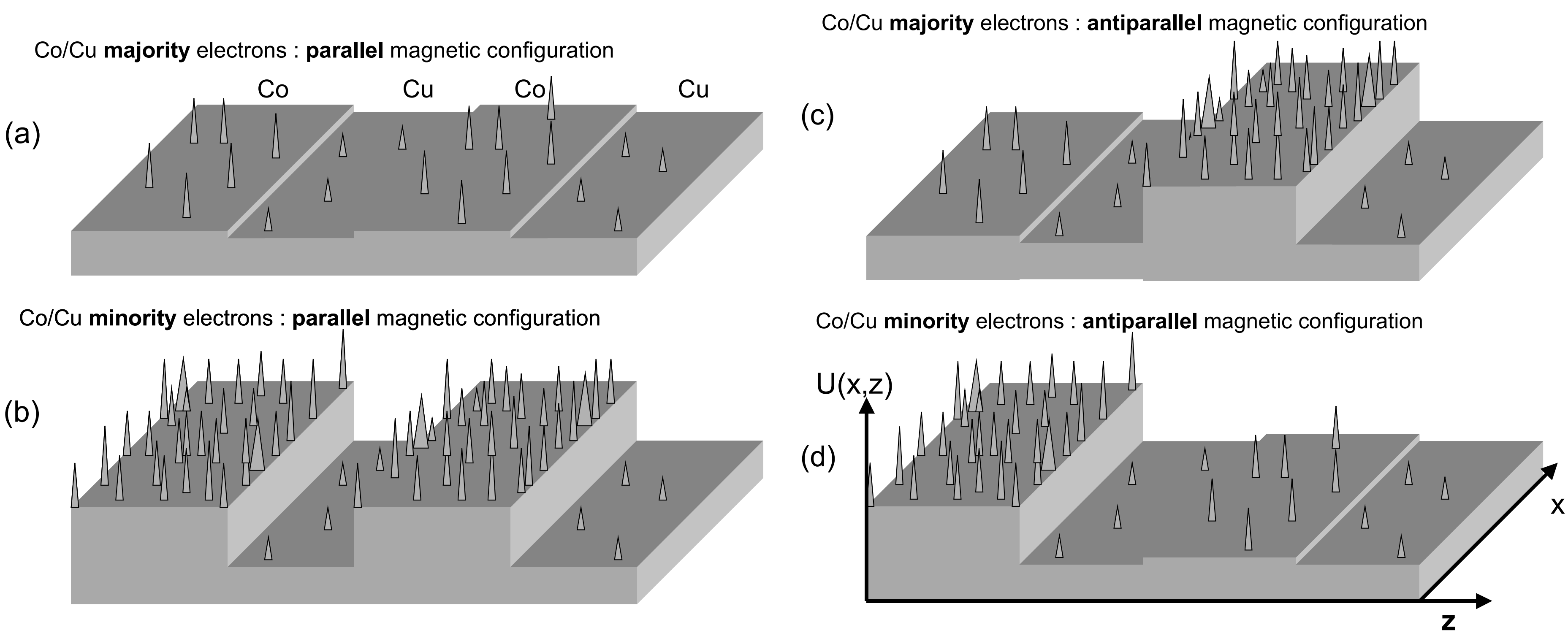

•<u>Lattice potential modulation</u> due to difference between Fermi energy and bottom of conduction band (reflection, refraction)

•<u>Spin-dependent scattering</u> on impurities, interfaces or grain boundaries (Dominant effect in GMR)

Simple model of Giant Magnetoresistance

Parallel config

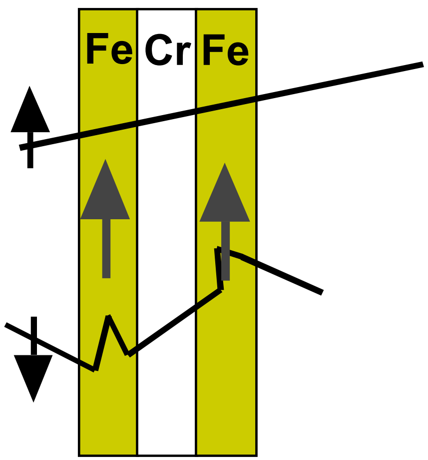

Antiparallel config

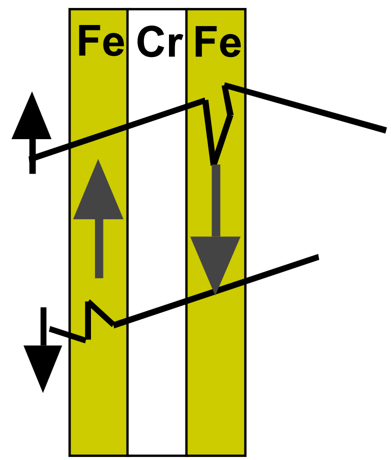

$$\frac{\Delta\rho}{\rho_{ap}} = \left(\frac{\rho_{\uparrow} - \rho_{\downarrow}}{\rho_{\uparrow} + \rho_{\downarrow}}\right)^2 = \left(\frac{\alpha - 1}{\alpha + 1}\right)^2$$

Equivalent resistances :

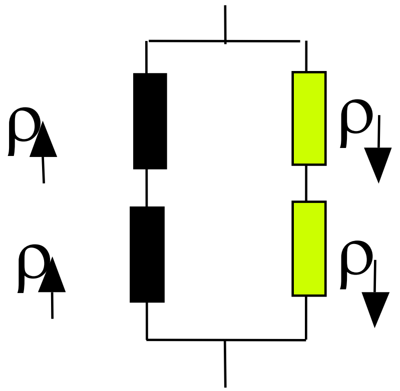

$$\rho_P = \frac{2\rho_{\uparrow}\rho_{\downarrow}}{(\rho_{\uparrow} + \rho_{\downarrow})}$$

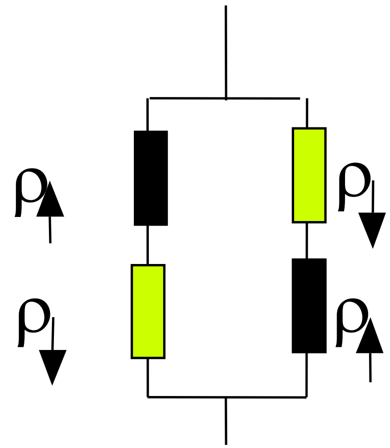

$$\rho_{AP} = \frac{(\rho_{\uparrow} + \rho_{\downarrow})}{2}$$

$$\alpha = \frac{\rho_{\uparrow}}{\rho_{\downarrow}}$$

Key role of scattering contrast α

Approach initiated by Camley and Barnas, PRL, 63, 664 (1989)

Gas of independent particles described by distribution f(r, v, t), submitted to force field **F** (=-e**E** for electrons in electrical field E).

Time evolution of the distribution described by Boltzman equation:

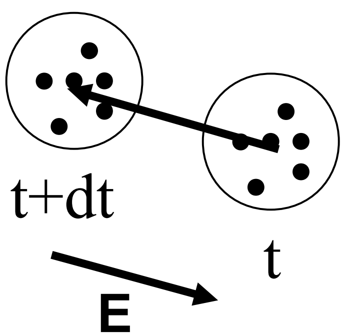

Equilibrium function conserved in a volume element d**r**d**v** along a flow line.

In presence of scattering, $$\frac{df}{dt} = \left(\frac{df}{dt}\right)_F - \left(\frac{df}{dt}\right)_{scattering} = 0$$

Balance between acceleration due to force and relaxation due to scattering

$$\left(\frac{df}{dt}\right)_F = \frac{\partial f}{\partial t} + \frac{\partial f}{\partial x}.v_x + \frac{\partial f}{\partial y}.v_y + \frac{\partial f}{\partial z}.v_z + \frac{\partial f}{\partial v_x}.a_x + \frac{\partial f}{\partial v_y}.a_y + \frac{\partial f}{\partial v_z}.a_z$$

$$= \frac{\partial f}{\partial t} + \vec{v}.\vec{\nabla}_{\vec{r}} f + \vec{a}.\vec{\nabla}_v f \qquad \text{with} \qquad m\vec{a} = \vec{F}$$

$$\left(\frac{df}{dt}\right)_F = \left(\frac{df}{dt}\right)_{scatt} = \frac{\partial f}{\partial t} + \vec{v}.\vec{\nabla}_{\vec{r}} f + \frac{\vec{F}}{m}.\vec{\nabla}_v f$$

In stationary regime, $\frac{\partial f}{\partial t} = 0$

In single relaxation time approximation (τ) $\left(\frac{df}{dt}\right)_{scatt} = \frac{-\left(f - f^0\right)}{\tau}$

Where f^0 is the equilibrium distribution (Fermi Dirac for electrons).

Boltzmann equation for electron gas in electrical field **E**:

$$\vec{v}.\vec{\nabla}_{\vec{r}} f + \frac{-e\vec{E}}{m}.\vec{\nabla}_v f = \frac{-\left(f - f^0\right)}{\tau}$$

Modeling current transport in bulk metals

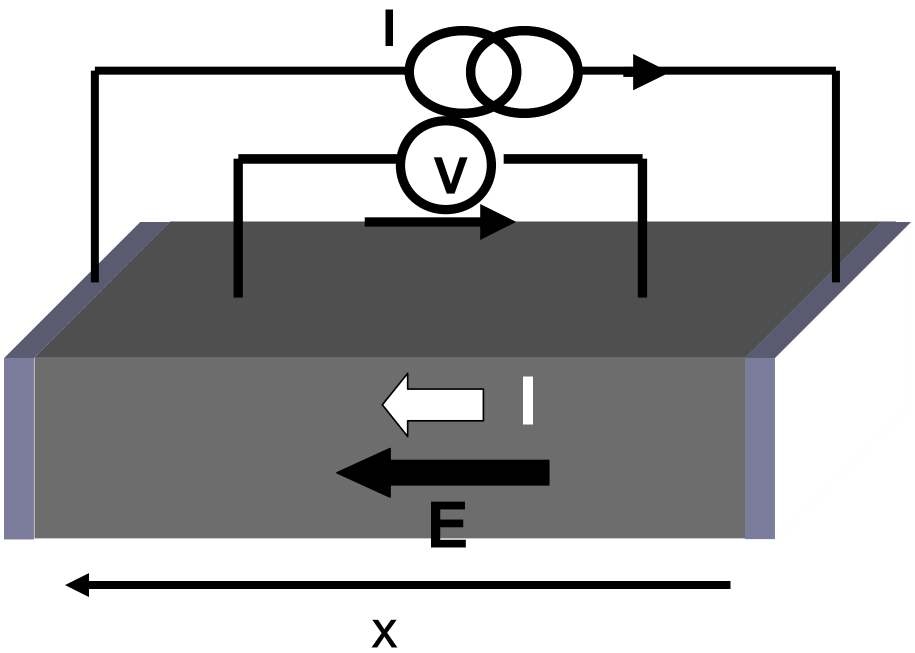

$$f(\vec{r},\vec{v}) = f_0(\vec{r},\vec{v}) + g(\vec{r},\vec{v})$$

Fermi-Dirac

Perturbation due to electric field

$$f_0(\vec{r},\vec{v}) = \frac{1}{\exp\left(\frac{\varepsilon-\varepsilon_F}{k_B T}\right)+1}$$

$$\vec{v}.\vec{\nabla}_{\vec{r}} f + \frac{-e\vec{E}}{m}.\vec{\nabla}_v f = \frac{-\left(f-f^0\right)}{\tau}$$

Spatially homogeneous transport $\vec{\nabla}_{\vec{r}} f = 0$

$$g(v_x) = \frac{eE_x\tau}{m}\frac{\partial f_0}{\partial v_x}$$

In k-space, shift in Fermi surface by

$$\hbar\Delta k = -eE_x\tau$$

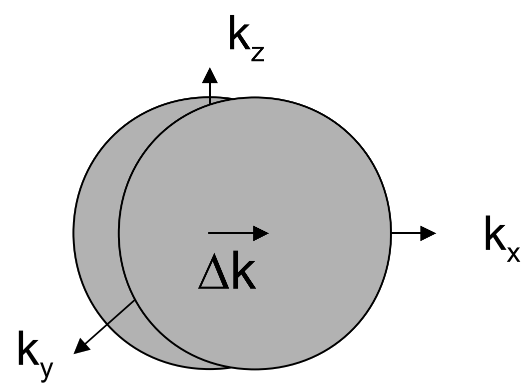

Current density:

$$j = -e\int v_x g(\vec{v}) d^3 v$$

$$j = \frac{ne^2\tau}{m} E = \sigma E = \frac{1}{\rho} E$$

$$\sigma = \frac{ne^2\tau}{m}$$

Well-known expression of conductivity in Drude model

n=density of conduction electrons

n~1/atom in noble metals such as Cu, Ag, Au
n~0.6/atom in metals such as Ni, Co, Fe

Typical resistivity of sputtered metals

Material	Measured resistivity 4K/300K
Cu[a]	0.5-0.7μΩ.cm 3-5
Ag[f]	1μΩ.cm 7
Au[g]	2μΩ.cm 8
$Pt_{50}Mn_{50}$[e]	160μΩ.cm 180
$Ni_{80}Cr_{20}$[e]	140μΩ.cm 140
Ru[c]	9.5-11μΩ.cm 14-20

Material (ferro)	Measured resistivity 4K/300K
$Ni_{80}Fe_{20}$[a]	10-15μΩ.cm 22-25
$Ni_{66}Fe_{13}Co_{21}$[b]	9-13μΩ.cm 20-23
Co[a,d]	4.1-6.45μΩ.cm 12-16
$Co_{90}Fe_{10}$[h]	6-9μΩ.cm 13-18
$Co_{50}Fe_{50}$[h]	7-10μΩ.cm 15-20

Thermal variation of resistivity due to phonon scattering and magnon scattering (in magnetic metals)

Modeling current transport in metallic thin films

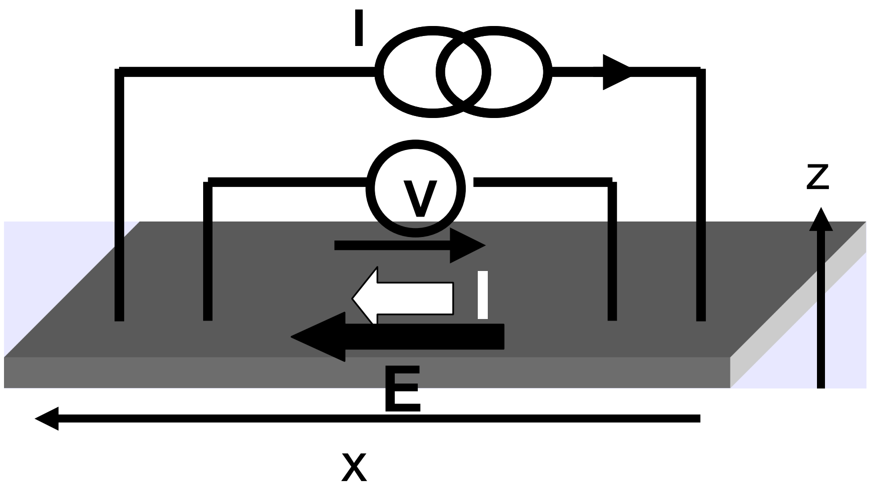

$$f(\vec{r},\vec{v}) = f_0(\vec{r},\vec{v}) + g(\vec{r},\vec{v})$$

$$\vec{v}.\vec{\nabla}_{\vec{r}} f + \frac{-e\vec{E}}{m}.\vec{\nabla}_v f = \frac{-\left(f - f^0\right)}{\tau}$$

Due to scattering at outer surfaces, the perturbation g is no longer homogeneous: g(z)

$$\frac{\partial g(z,v)}{\partial z} + \frac{g(z,v)}{\tau v_z} = \frac{eE}{m v_z}\frac{\partial f^0(v)}{\partial v_x}$$

$$\tau = \frac{\lambda}{v_F}$$

$\lambda =$ elastic mean free path

Integration constants determined from boundary conditions

General solution :

$$g_\pm(z,v) = eE\tau\ v_x \frac{\partial f_0}{\partial \varepsilon}\left[1 - A_\pm \exp\left(\mp \frac{z}{\tau |v_z|}\right)\right]$$

+(-) refer to electrons traveling towards z>0 (z<0)

Boundary conditions for a thin film :

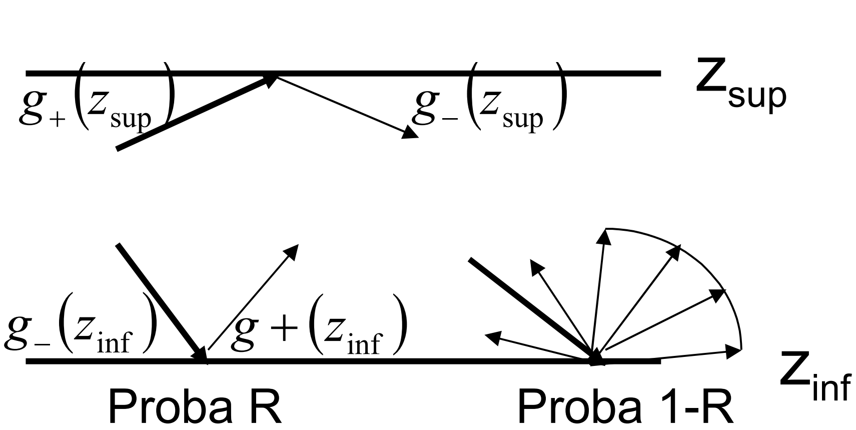

$$\begin{cases} g_-(z_{sup}) = R g_+(z_{sup}) \\ g_+(z_{inf}) = R g_-(z_{inf}) \end{cases}$$

Proba of **specular reflection** R
Proba of **diffuse reflection** 1-R

Two boundary conditions, two unknowns A+, A-, solvable problem

Current density:

$$j(z) = e\int v_x g^{\sigma}(v_z, z) d^3v$$

$$j(z) \propto \int_0^1 (1-\mu^2)\left[2 - A_+ \exp\left(\frac{-t}{\lambda\mu}\right) - A_- \exp\left(\frac{t}{\lambda\mu}\right)\right] d\mu$$

t=layer thickness, μ= cosine of electron incidence

Modeling current transport in metallic thin films (cont'd)

$$G = G_0 - G_1$$

$$G_0 = \frac{ne^2\lambda}{v_F m} t = \sigma\, t$$

thickness

Same conductance as in bulk

$$G_1 = \frac{3\lambda}{4\rho}\int_0^1 d\mu\left(1-\mu^2\right)\mu\left\{A_+\left[1-\exp\left(\frac{-t}{\lambda\mu}\right)\right]+A_-\left[1-\exp\left(\frac{t}{\lambda\mu}\right)\right]\right\}$$

G_1 contains all finite size effects.

Characteristic length in current-in-plane transport=elastic mfp

j(z)

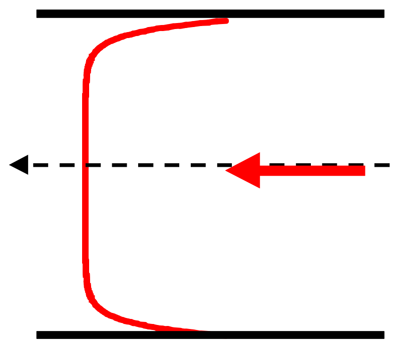

Assuming diffuse surface scatt

Fuchs-Sondheimer approximate expressions:

$$\rho = \frac{mv_F}{ne^2}\left(\frac{1}{\lambda}+\frac{3}{8t}\right) \quad \text{for } \lambda << \text{t}$$

$$\rho = \frac{4mv_F}{3ne^2}\left(\frac{1}{t\left\{\ln\left(\lambda/t\right)+0.423\right\}}\right) \quad \text{for } \lambda >> \text{t}$$

Models in spintronics (Part I)

OUTLINE :

Spin-dependent transport in metallic magnetic multilayers

-Introduction to spin-electronics

-Spin-dependent scattering in magnetic metal

-Current-in-plane Giant Magnetoresistance

-Modelling CIP Giant Magnetoresistance

-Current-perpendicular-to-plane Giant Magnetoresistance

-Spin accumulation, spin current, 3D generalization.

Modeling current in plane GMR in metallic multilayers

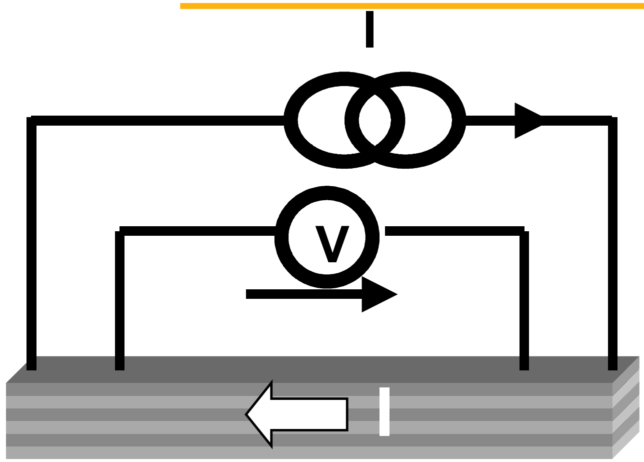

CIP

Same as for thin films but separately considering spin↑ and spin ↓ electrons and solving the Boltzmann equation within each layer with appropriate boundary conditions.

- Bulk spin-dependent scattering described by spin dependent mfp λ^σ
- Interfacial scattering described by spin dependent R^σ and T^σ

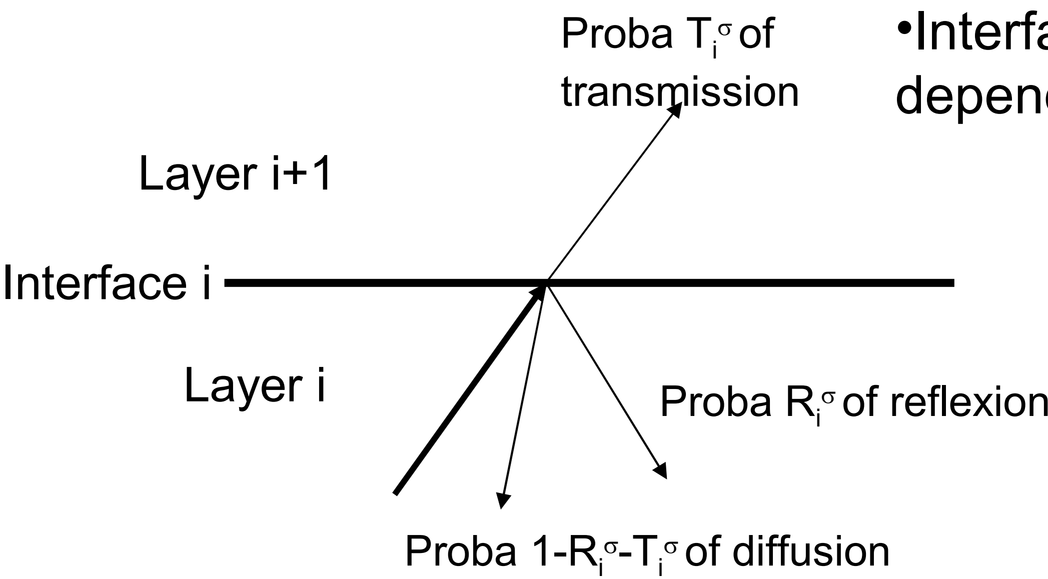

$$g^{\sigma}_{i+1,+} = T^{\sigma}_{i}\, g^{\sigma}_{i,+} + R^{\sigma}_{i}\, g^{\sigma}_{i+1,-}$$

$$g^{\sigma}_{i,-} = T^{\sigma}_{i}\, g^{\sigma}_{i+1,-} + R^{\sigma}_{i}\, g^{\sigma}_{i,+}$$

Modeling current in plane GMR in metallic multilayers

$$G = G_0 - G_1$$

$$G_0 = e^2 \sum_{i=1,\uparrow\downarrow}^{N} \frac{\lambda_i^\sigma n_i^\sigma t_i}{v_F m_i} = \sum_{i=1,\uparrow\downarrow}^{N} t_i / \rho_i^\sigma$$

Same conductance as if all layers were connected in parallel

$$G_1 = \frac{3\lambda_i^\sigma}{4\rho_i^\sigma} \sum_{\uparrow\downarrow,i} \int_0^1 d\mu \left(1-\mu^2\right)\mu \left\{ A_{i,+}^\sigma \left[1-\exp\left(\frac{-t_i}{\lambda_i^\sigma \mu}\right)\right] + A_{i,-}^\sigma \left[1-\exp\left(\frac{t_i}{\lambda_i^\sigma \mu}\right)\right]\right\}$$

G_1 contains all finite size effects and is responsible for GIP GMR.

To obtain the GMR, G_1 is calculated in parallel and antiparallel configurations.

In AP configuration, $\lambda^\uparrow, \mathrm{R}^\uparrow, \mathrm{T}^\uparrow$ and $\lambda^\downarrow, \mathrm{R}^\downarrow, \mathrm{T}^\downarrow$ are inverted in every other layer.

CIP GMR comes from second order effect in conductivity (in contrast to CPP GMR)

Characteristic lengths in CIP GMR are the elastic mean-free paths

Influence of feromagnetic layer thickness on GMR in spin-valves

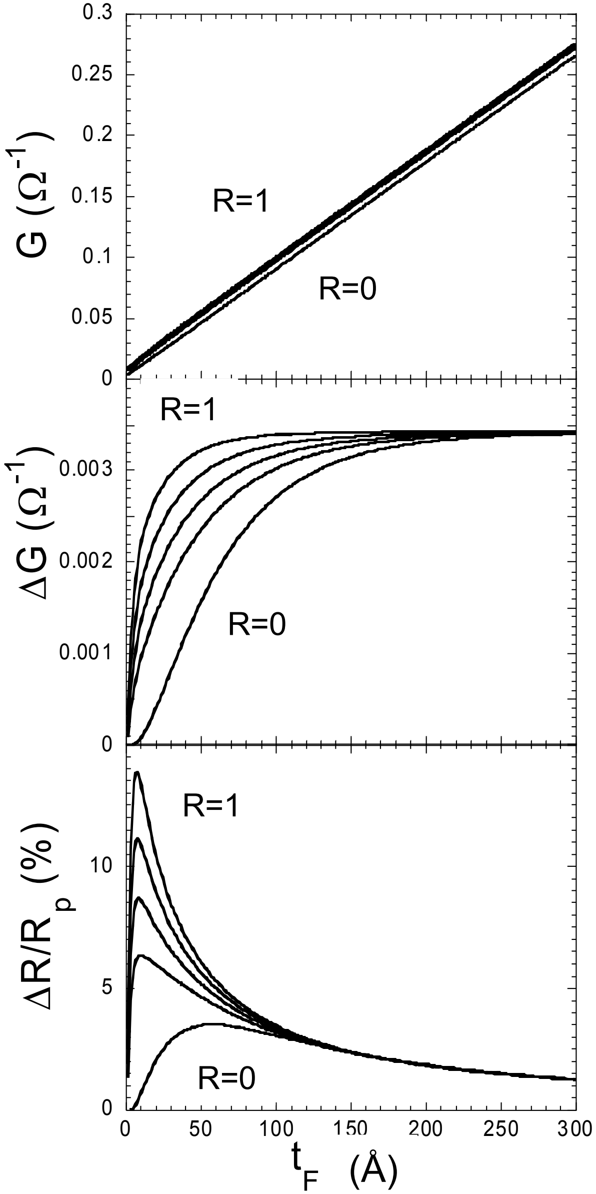

Example of calculated CIP curves
For a NiFe t_{NiFe}/Cu 2nm/NiFe t_{NiFe}
Sandwich.
R=coeff of specular reflection at lateral edges

$$\lambda_{\uparrow}^{NiFe} = 7nm, \lambda_{\downarrow}^{NiFe} = .8nm,$$

$$\lambda^{Cu} = 12nm,$$

$$T_{\uparrow}^{NiFe/Cu} = T_{\downarrow}^{NiFe/Cu} = 0.9$$

Absolute change of sheet conductance
most intrinsic measure of CIP GMR

F/Cu25Å/NiFe50Å/FeMn100Å

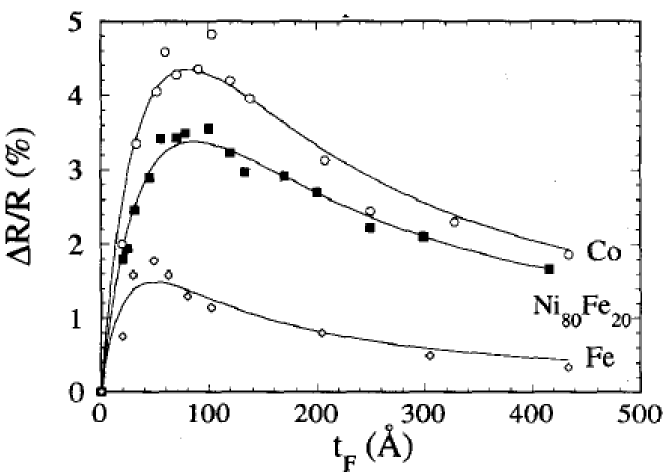

B.Dieny
JMMM (1994)

Influence of nature of ferro materials on GMR in spin-valves

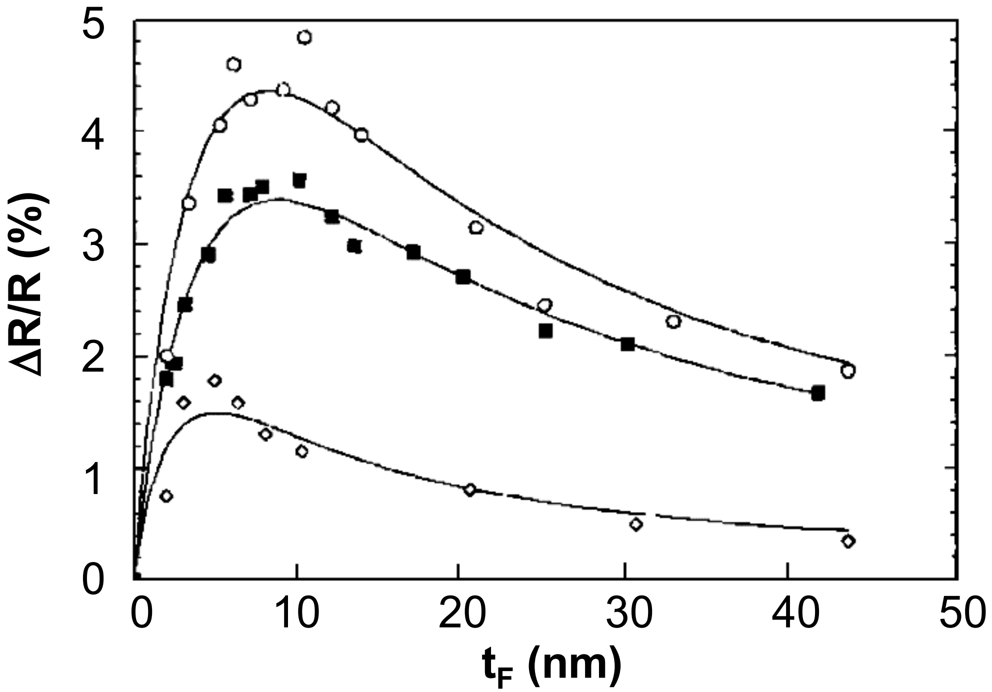

F tF/Cu 2.5nm/NiFe 5nm/FeMn 10nm,
with F=Ni80Fe20, Co and Fe (Dieny, 1991).

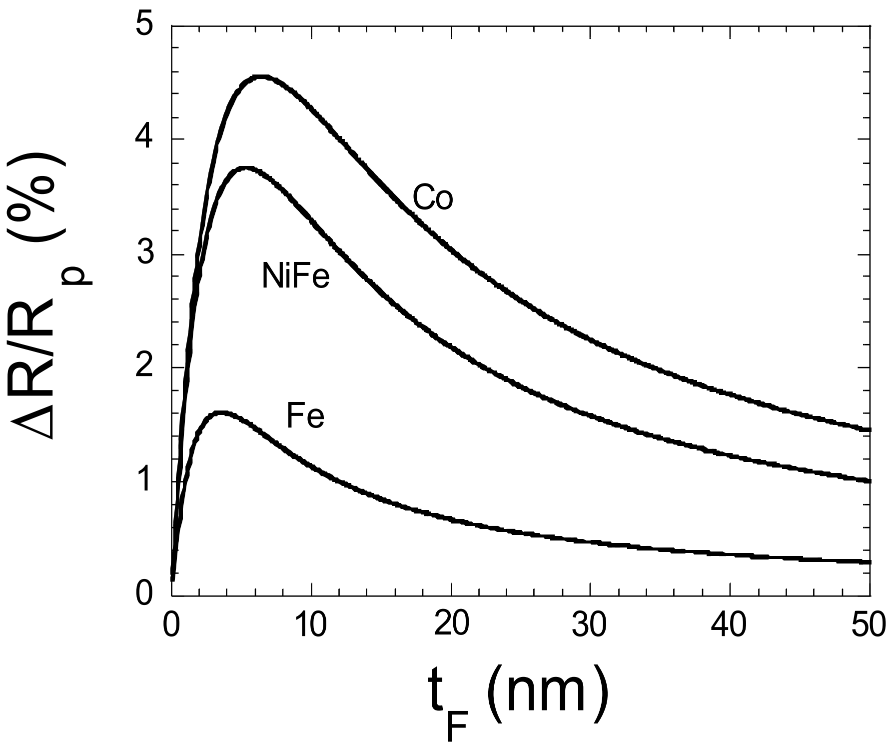

F t_F/Cu 2.5nm/NiFe5nm/FeMn 10nm

$$\lambda^{\uparrow}_{NiFe} = 7nm, \lambda^{\downarrow}_{NiFe} = 0.7nm, T^{\uparrow}_{NiFe/Cu} = 0.85, T^{\downarrow}_{NiFe/Cu} = 0.30,$$

$$\lambda^{\uparrow}_{Co} = 9nm, \lambda^{\downarrow}_{Co} = 0.9nm, T^{\uparrow}_{Co/Cu} = 0.95, T^{\downarrow}_{Co/Cu} = 0.30,$$

$$\lambda^{\uparrow}_{Fe} = 4.5nm, \lambda^{\downarrow}_{Fe} = 4.5nm, T^{\uparrow}_{Fe/Cu} = 0.70, T^{\downarrow}_{Fe/Cu} = 0.30.$$

Influence of non-magnetic spacer layer thickness on GMR in spin-valves

NiFe 3nm/Cu t_{Cu}/NiFe 3nm

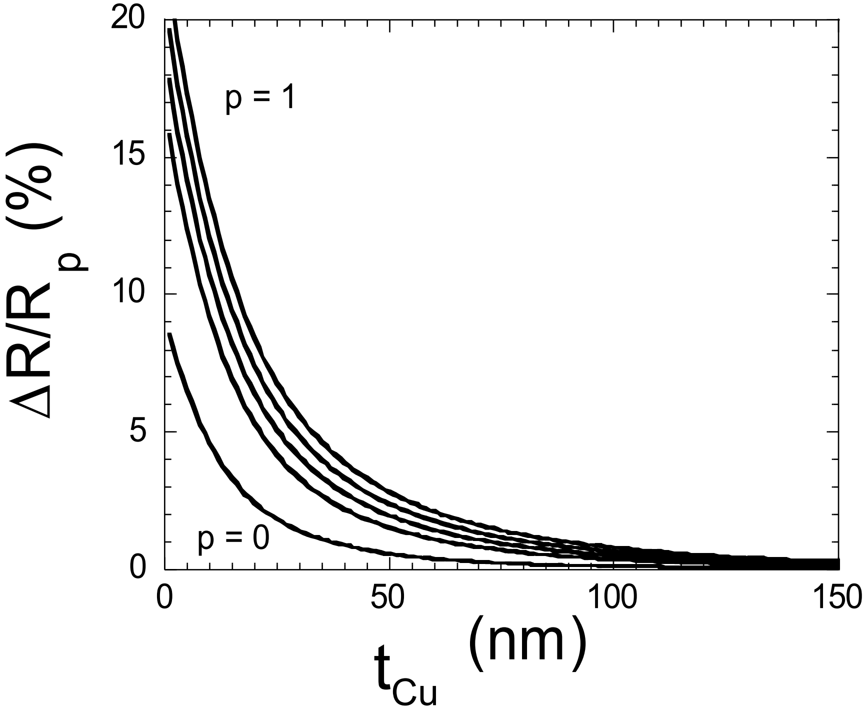

Semi-classical theory

NiFe50Å/NM t_{NM} /NiFe50Å/FeMn100Å

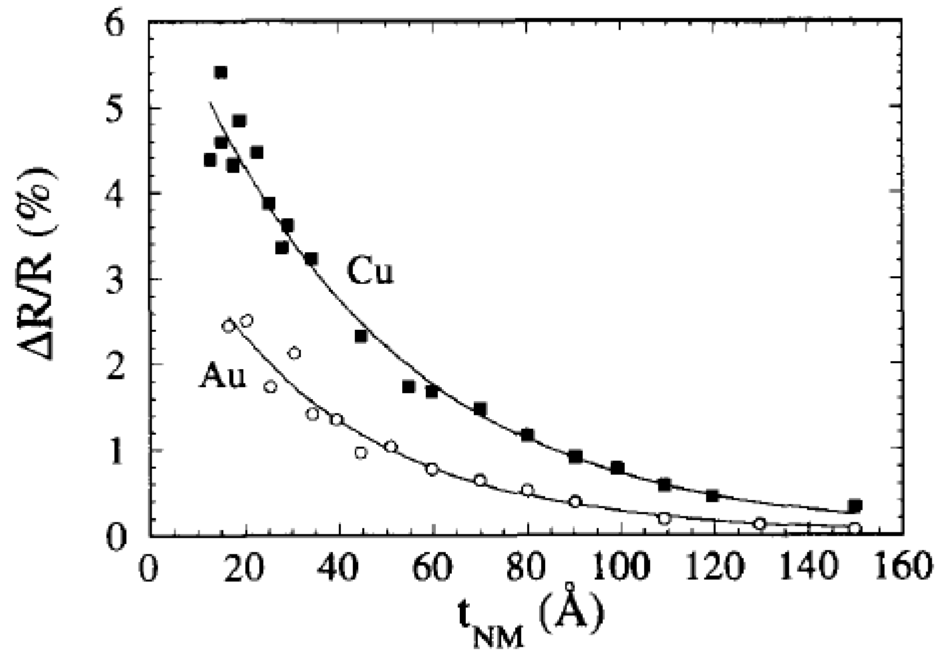

Experiments

B.Dieny JMMM (1994)

Two effects as t_{NM} increases:

- Reduced number of electrons travelling from one ferro layer to the other
- Increasing shunting of the current in the spacer layer

Local current density and magnetic field due to current in a CIP spin-valve

$$j(z) \propto \sum_{\uparrow\downarrow,i} \int_0^1 \left(1-\mu^2\right)\left[2 - A_{i,+}^{\sigma} \exp\left(\frac{-t_i}{\lambda_i^{\sigma}\mu}\right) - A_{i,-}^{\sigma} \exp\left(\frac{t_i}{\lambda_i^{\sigma}\mu}\right)\right] d\mu$$

Oersted field due to sense current in a CIP spin-valves

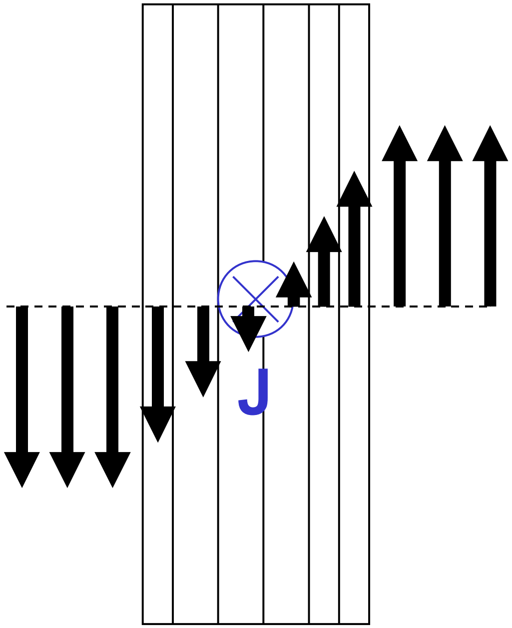

$$B(z) = \mu_0 \int_0^z j(z')dz' + cst$$

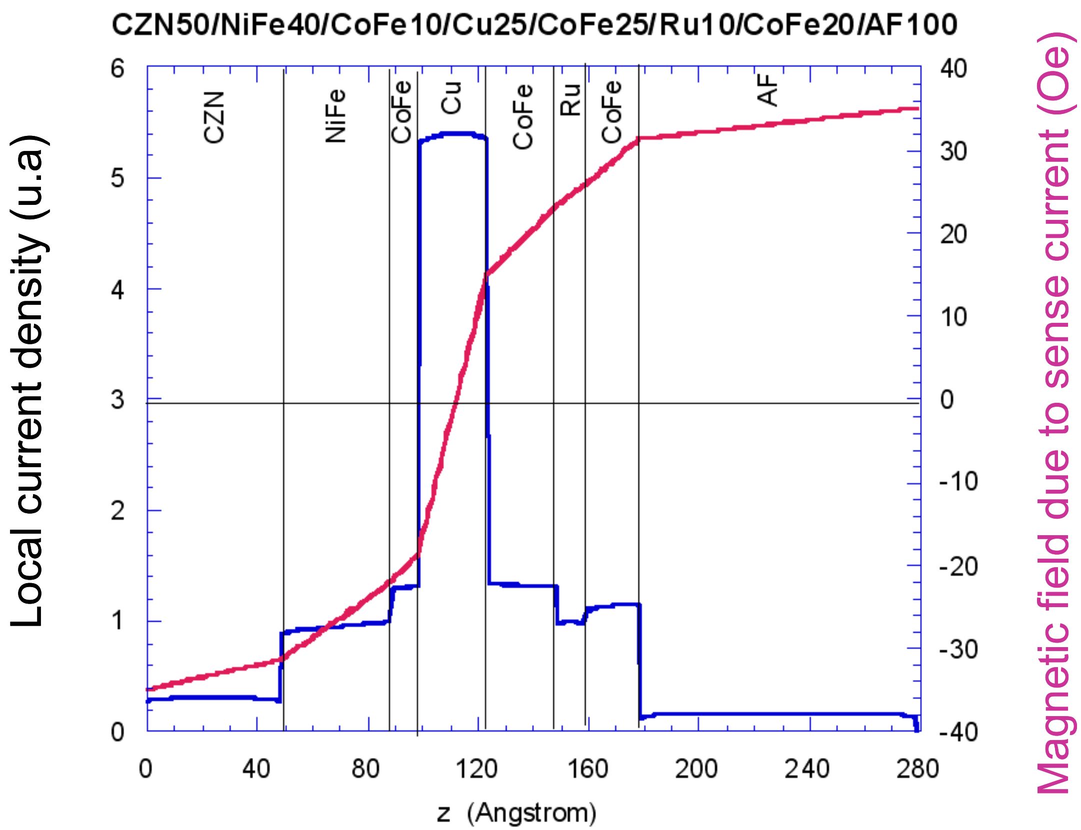

$<j>=2.10^7 A/cm^2$

Oe field plays an important role in the bias of spin-valve heads

Vertical head with CIP MR reader

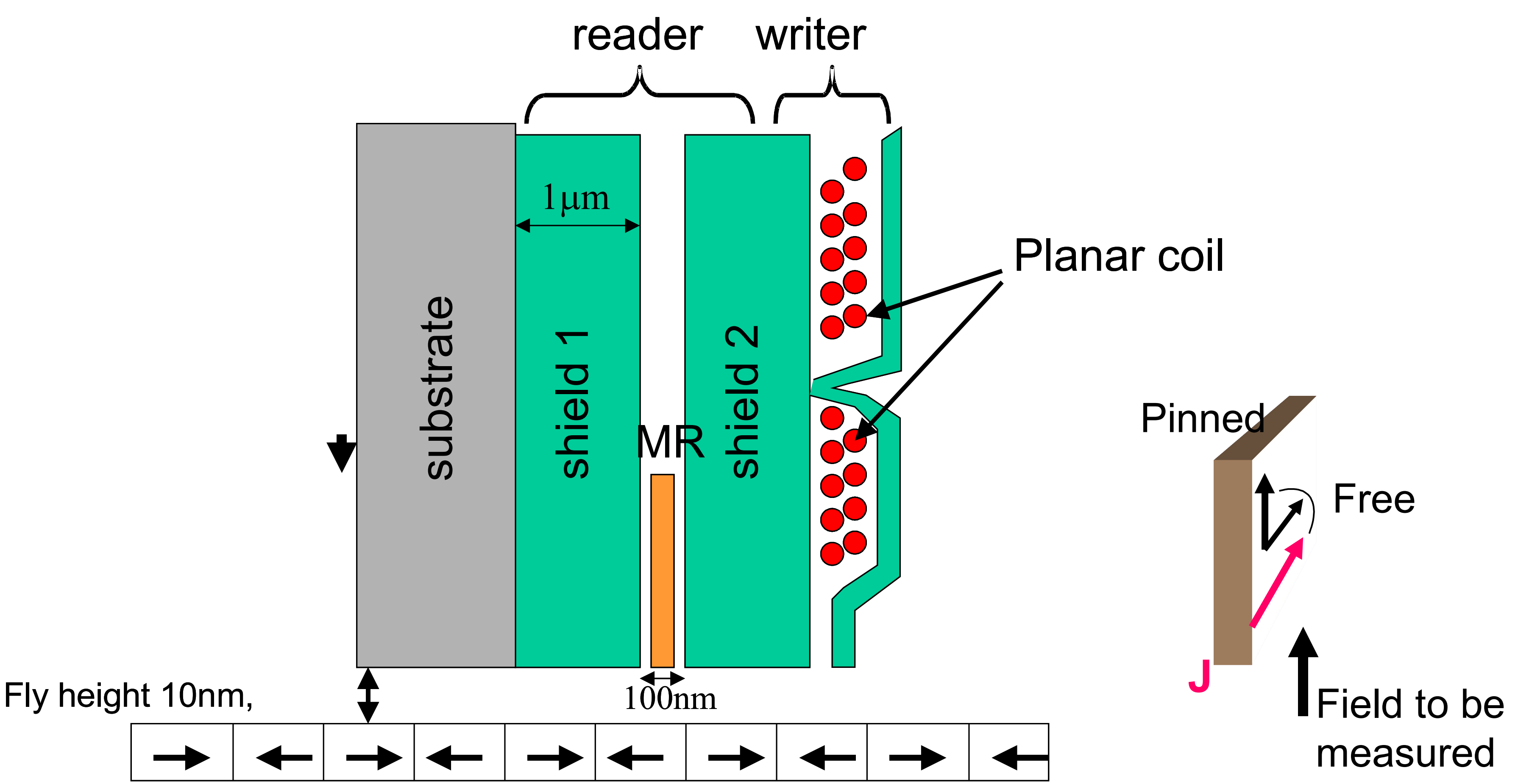

disk rotating at 5000 to 10000 rpm.

Linear response of spin-valves MR heads

Energy terms influencing the orientation of free layer magnetization:

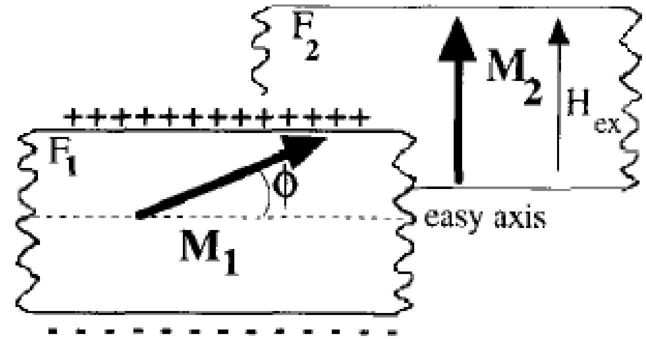

•Zeeman coupling to H, to coupling field through Cu spacer and to Oersted field:

$$E = -M_1(H + H_{SV} + H_J).\sin(\phi)$$

•Uniaxial and shape anisotropy

$$E = -(K + NM_s^2).\cos^2(\phi)$$

•Dipolar coupling with pinned layer

$$E = M_1 H_{dip}.\sin(\phi)$$

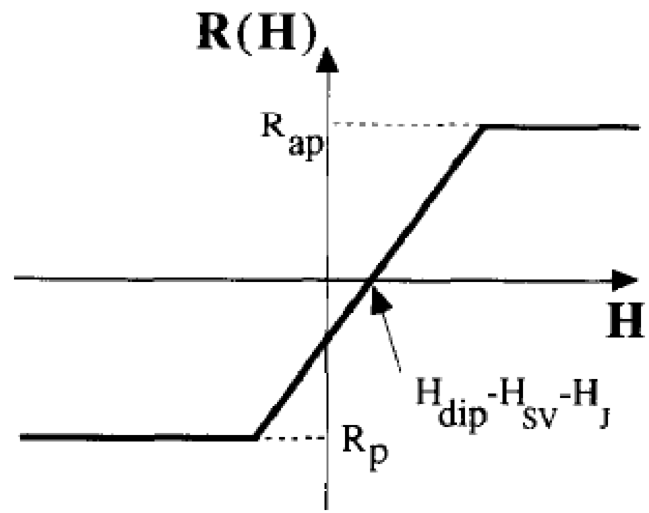

Minimizing energy yields $\sin(\phi)$ linear in H.
Since R varies as $\vec{M}_1.\vec{M}_2 \,\alpha\, \sin(\phi)$
linear R(H)

$$R(H) = R_P + (R_{AP} - R_P)\left[1 - \frac{M_1\left(H + H_{SV} + H_I - H_{dip}\right)}{2\left(K + NM_1^2\right)}\right]$$

Experimental optimization of spin-valves

Spin-valves greatly optimized in 1994-2003 for HDD MR heads but replaced in 2004 by TMR heads

NiFeCr/PtMn 120Å/ CoFe 15Å /Ru 7Å/CoFe 5Å/NOL/CoFe 15Å /Cu 20Å/CoFe10Å/NiFe 20Å /NOL

pinned

soft

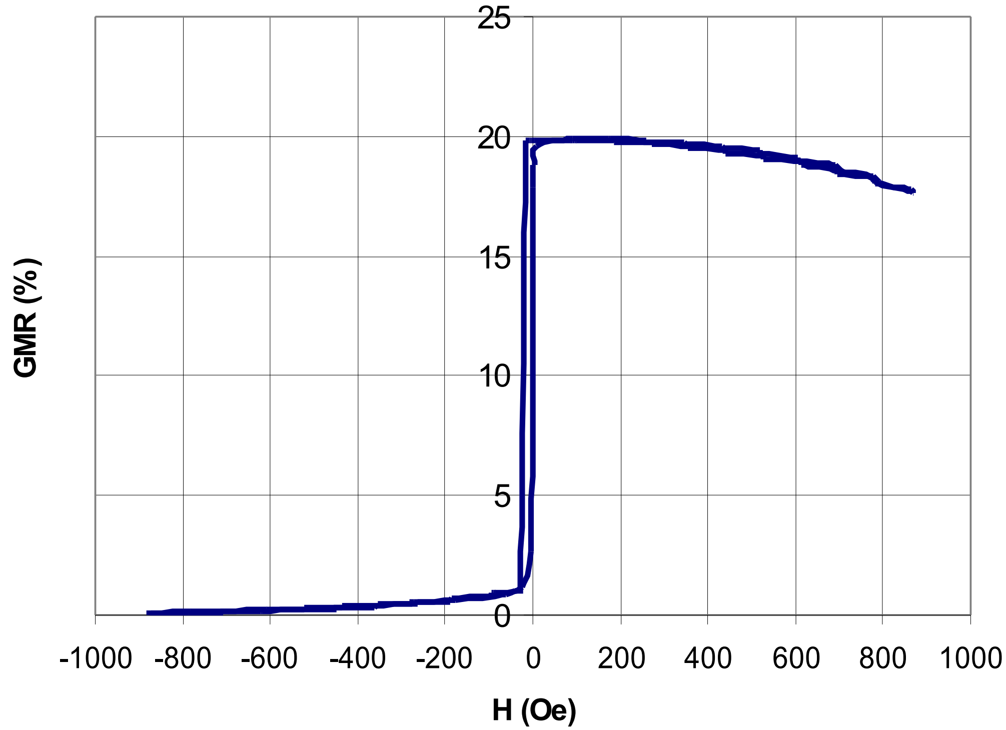

GMR amplitude significantly improved by increasing specular reflection at boundaries of active part of the spin-valve //(pinned/spacer/free)//

Conclusion on CIP GMR :

CIP GMR well modeled by semi-classical Boltzmann theory.

Local conductivity can only vary on length scale of the order of the elastic mean free path.

Quantum mechanical theory of CIP transport were proposed to properly take into account the quantum confinement/reflection/refraction effects induced by lattice potential modulation. Predictions of oscillations in conductivity and GMR versus thickness but hardly seen in experiments due to interfacial roughness

CIP GMR amplitude up to 20% in specular spin-valves.

Spin-valves were used in MR heads of hard disk drives from 1998 to 2004. Later on, they were replaced by Tunnel MR heads.

Models in spintronics (Part I)

OUTLINE :

Spin-dependent transport in metallic magnetic multilayers

-Introduction to spin-electronics

-Spin-dependent scattering in magnetic metal

-Current-in-plane Giant Magnetoresistance

-Modelling CIP Giant Magnetoresistance

-Current-perpendicular-to-plane Giant Magnetoresistance

-Spin accumulation, spin current, 3D generalization.

Current Perpendicular to Plane GMR

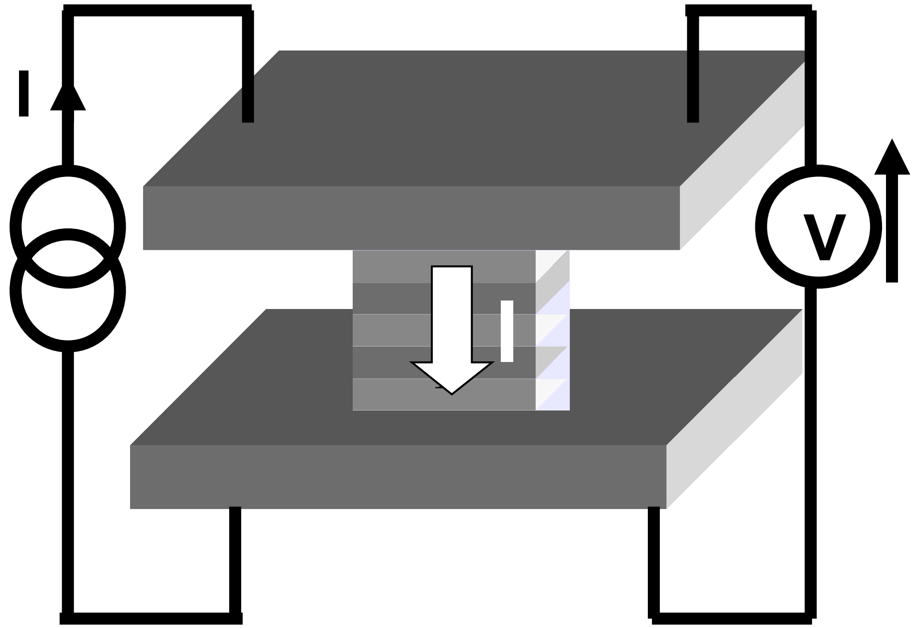

Much more difficult to measure,
Either on macroscopic samples (0.1mm diameter) with superconducting leads ($R \sim \rho$. thickness / area $\sim 10^{-5}\Omega$)
or on patterned microscopic pillars of area <μm^2 (R~ a few Ohms)

Serial resistance model for CPP-GMR

Without spin-filp, serial resistance network can be used for CPP transport

CPP transport through F/NM/F sandwich described by:

(a) Parallel magnetic configuration :

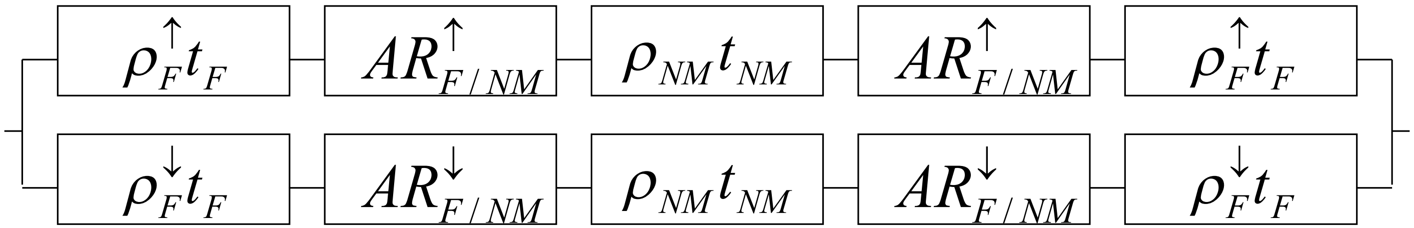

(b) Antiparallel magnetic configuration :

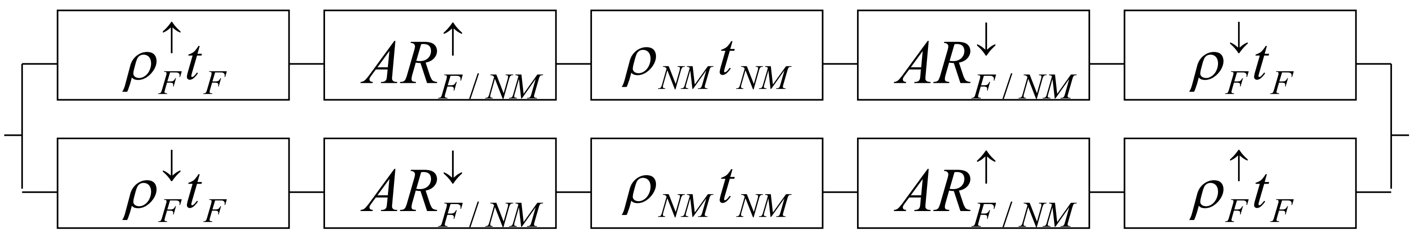

Parallel resistance model for CIP-GMR:

CIP GMR of (Co t_{Co}/Cu t_{Cu}) $_2$ multilayers

Parallel configuration : **Antiparallel configuration :**

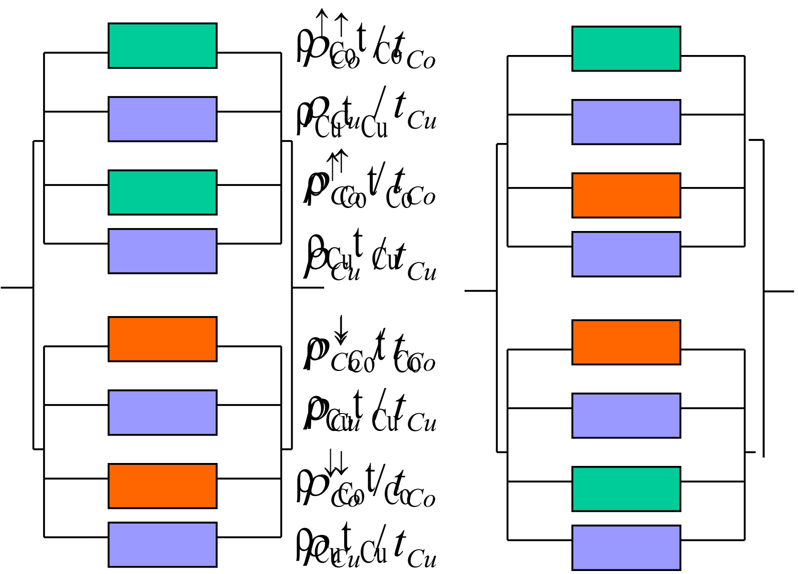

CIP GMR cannot be described
by a parallel resistance network only
(no change of R between parallel and
antiparallel magnetic configuration)

Serial resistance model for CPP-GMR:

CPP GMR of (Co t_{Co}/Cu t_{Cu}) $_2$ multilayers

Parallel magnetic configuration :

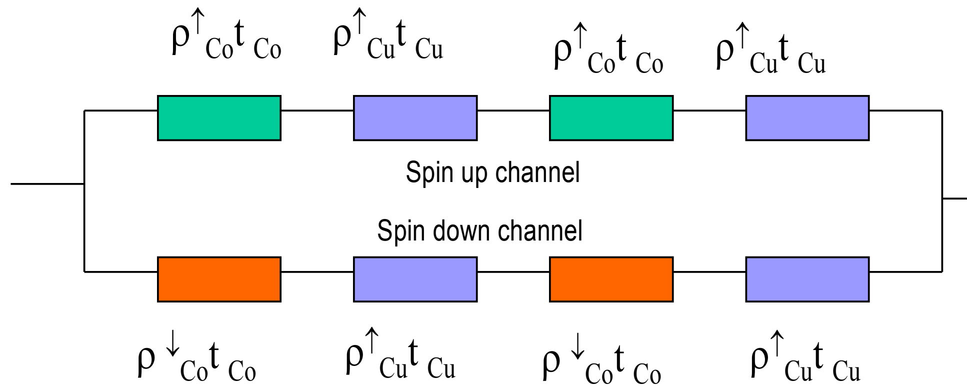

Antiparallel magnetic configuration :

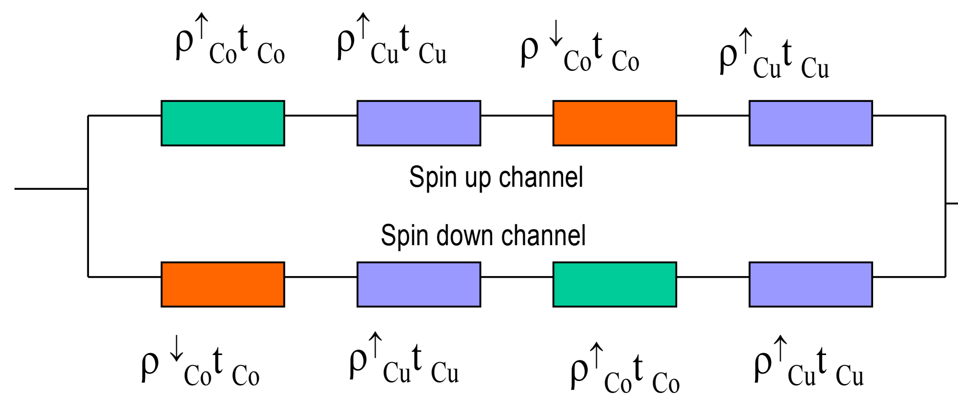

CPP GMR can be « qualitatively » described
by a serial resistance network
(without spin-flip, i.e. no mixing between up and down channels)

Spin accumulation – spin relaxation in CPP geometry

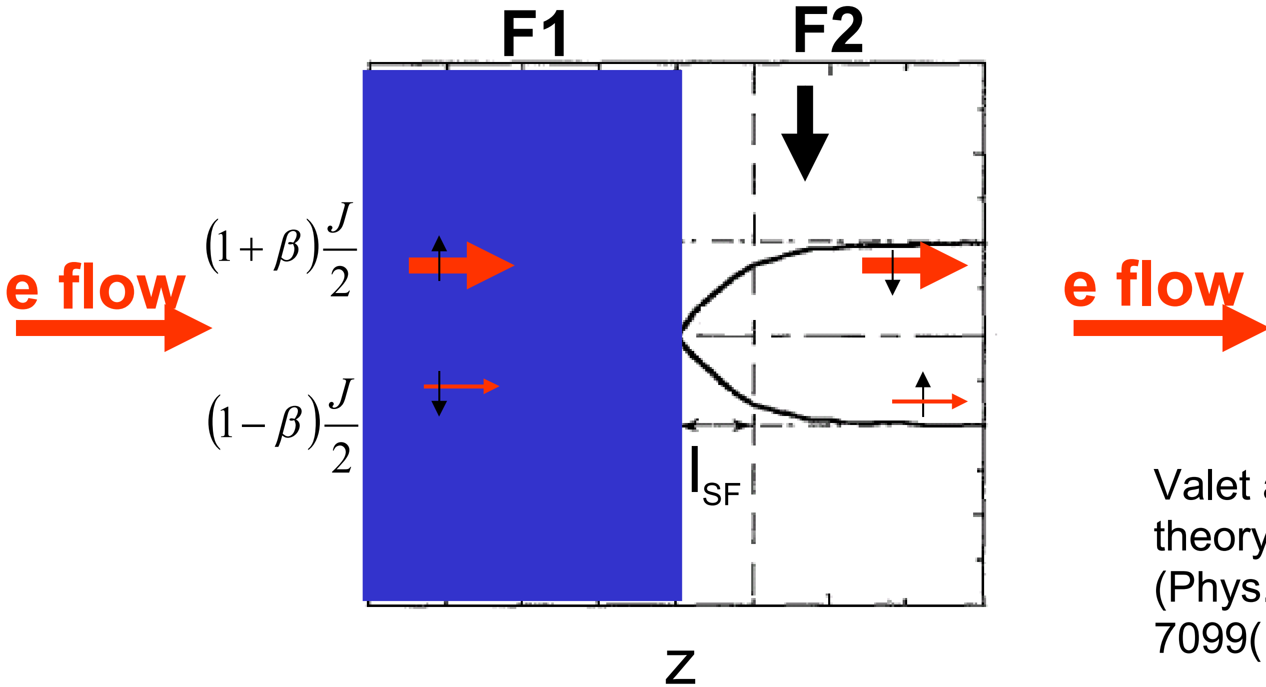

Valet and Fert theory of CPP-GMR (Phys.Rev.B48, 7099(1993))

In F1: Different scattering rates for spin ↑ and spin ↓ electrons
⇒ different spin ↑ and spin ↓ currents.
Larger scattering rates for spin ↓ : $J\uparrow >> J\downarrow$ far from the interface.

In F2: Larger scattering rates for spin ↑ : $J_{\downarrow} >> J_{\uparrow}$ far from the interface.

Majority of incoming spin ↑electrons, majority of outgoing spin↓ electrons

Building up of a spin↑accumulation around the interface balanced in steady state by spin-relaxation

Starting point : Valet and Fert theory of CPP-GMR (Phys.Rev.B48, 7099(1993))

μ_σ : spin-dependent chemical potential

In homogeneous material, $\mu=\varepsilon_F-e\phi$

Spin-relaxation at F↑/F↓ interface:

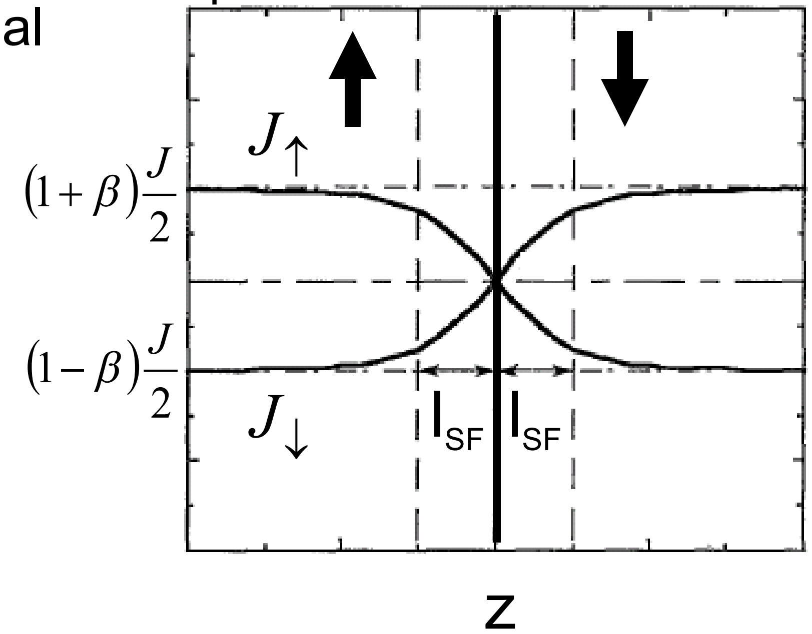

Spin-dependent current driven by $\vec{\nabla}\mu$

$$J_\sigma = \frac{1}{e\rho_\sigma}\frac{\partial \mu_\sigma}{\partial z}$$

Generalization of Ohm law

Spin relaxation :

$$e\rho_\sigma \frac{\partial J_\sigma}{\partial z} = \frac{\mu_\sigma - \mu_{-\sigma}}{2l_{SF}^2}$$

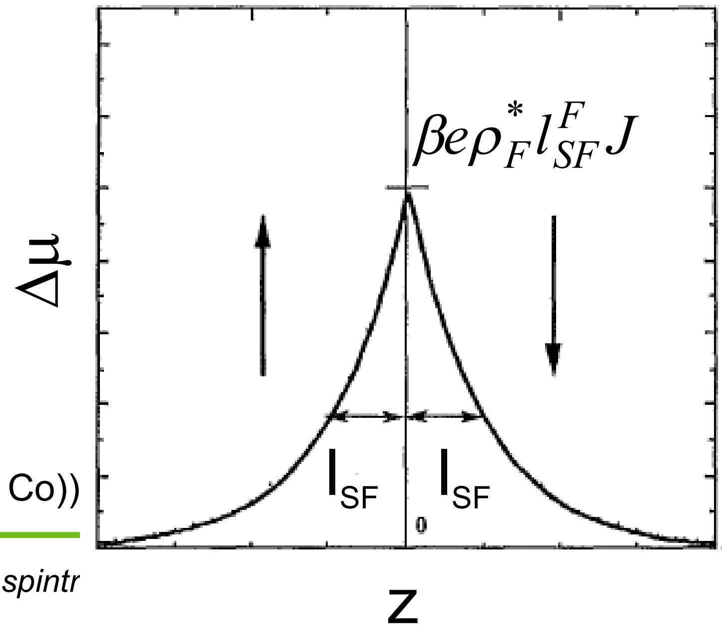

l_{SF}=spin-diffusion length (~5nm in NiFe, ~20nm in Co))

Interfacial boundary conditions

$$\mu_{i+1}^{\uparrow(\downarrow)}\left(z_{i+1}\right)-\mu_{i}^{\uparrow(\downarrow)}\left(z_{i+1}\right)=r_{i+1}^{\uparrow(\downarrow)}J_{i}^{\uparrow(\downarrow)}\left(z_{i+1}\right)$$ (Ohm law at interfaces)

$$J_{i+1}^{\uparrow(\downarrow)}\left(z_{i+1}\right)=J_{i}^{\uparrow(\downarrow)}\left(z_{i+1}\right)$$ (if no interfacial spin-flip is considered)

Note: Interfacial spin memory loss can be introduced by :

$$J_{i+1}^{\uparrow(\downarrow)}\left(z_{i+1}\right)=\delta\, J_{i}^{\uparrow(\downarrow)}\left(z_{i+1}\right)$$

30% memory loss as at Co/Cu interface yields δ=0.7

Input microscopic transport parameters to describe macroscopic CPP properties

Within each layer :

-The measured resistivity ρ.

-The scattering asymmetry β.

-The spin diffusion length l_{sf}.

$$\rho_{\uparrow(\downarrow)} = 2\rho^*[1-(+)\beta]$$

$$\rho_{measured} = \frac{\rho_\uparrow \rho_\downarrow}{\rho_\uparrow + \rho_\downarrow} = \rho^*(1-\beta^2)$$

At each interface :

-The measured interfacial area*resistance product $r_{measured}$

-The interfacial scattering asymmetry γ.

$$r_{\uparrow(\downarrow)} = 2r^*[1-(+)\gamma]$$

$$r_{measured} = \frac{r_\uparrow r_\downarrow}{r_\uparrow + r_\downarrow} = r^*(1-\gamma^2)$$

Examples of bulk parameters

Material	Measured resistivity 4K/ 300K	β Bulk scattering asymmetry	l_{SF}
Cu	0.5-0.7$\mu\Omega$.cm 3-5	0 0	500nm 50-200nm
Au	2$\mu\Omega$.cm 8	0 0	35nm 25nm
$Ni_{80}Fe_{20}$	10-15 22-25	0.73-0.76 0.70	5.5 4.5
$Ni_{66}Fe_{13}Co_{21}$	9-13 20-23	0.82 0.75	5.5 4.5
Co	4.1-6.45 12-16	0.27 – 0.38 0.22-0.35	60 25
$Co_{90}Fe_{10}$	6-9 13-18	0.6 0.55	55 20
$Co_{50}Fe_{50}$	7-10 15-20	0.6 0.62	50 15
$Pt_{50}Mn_{50}$	160 180	0 0	1 1
Ru	9.5-11 14-20	0 0	14 12

Examples of interfacial parameters

Material	Measured R.A interfacial resistance	γ Interfacial scattering assymetry
Co/Cu	0.21mΩ.μm^2 0.21-0.6	0.77 0.7
$Co_{90}Fe_{10}$/Cu	0.25-0.7 0.25-0.7	0.77 0.7
$Co_{50}Fe_{50}$/Cu	0.45-1 0.45-1	0.77 0.7
NiFe/Cu	0.255 0.25	0.7 0.63
NiFe/Co	0.04 0.04	0.7 0.7
Co/Ru	0.48 0.4	-0.2 -0.2
Co/Ag	0.16 0.16	0.85 0.80

Diffusion equation of spin-accumulation

Spin-dependent currents : $J_\sigma = \dfrac{1}{e\rho_\sigma}\dfrac{\partial \mu_\sigma}{\partial z}$ (generalized Ohm law in the bulk of the layer)

Spin relaxation : $e\rho_\sigma \dfrac{\partial J_\sigma}{\partial z} = \dfrac{\mu_\sigma - \mu_{-\sigma}}{2 l_{SF}^2}$

$\Rightarrow$ Diffusion equation diffusion for spin accumulation $\Delta\mu$ $\dfrac{\partial^2 \Delta\mu}{\partial z^2} = \dfrac{\Delta\mu}{l_{SF}^2}$

Solution within each layer:

$$\Delta\mu = A\exp\left(\frac{z}{l_{sf}}\right) + B\exp\left(-\frac{z}{l_{sf}}\right)$$

A, B integration constants determined from interfacial boundary conditions

$$J_\sigma = \frac{1}{\rho_\sigma}\left(-grad\varphi \pm \frac{1}{e}\frac{\partial \Delta\mu}{\partial z}\right)$$

Drift due to electrical field

Diffusion due to local spin accumulation

Final expression of CPP resistance for any multilayered structures (N layers) :

$$R_{CPP} = \sum_{i=1}^{N} \left(1-\beta_i^2\right)\rho_i^* d_i + r_i^*\left(1-\gamma_i\right)\left(1+\beta_i\right) +$$

$$+\frac{1}{J} A_i \left[\left(1-\beta_i\right)\left(1-e^{-\lambda_i}\right) + \frac{r_i\left(1-\gamma_i\right)}{\rho_i l_i}\right] e^{\frac{d_i}{l_i}} +$$

$$+\frac{1}{J} B_i \left[\left(1-\beta_i\right)\left(1-e^{-\lambda_i}\right) - \frac{r_i\left(1-\gamma_i\right)}{\rho_i l_i}\right] e^{-\frac{d_i}{l_i}}$$

Where : $\begin{pmatrix} A_{i+1} \\ B_{i+1} \end{pmatrix} = \hat{\rho}_i \begin{pmatrix} A_i \\ B_i \end{pmatrix} + J\hat{J}_i$ with : $\hat{\rho}_i = \begin{pmatrix} \rho_i^{AA} & \rho_i^{AB} \\ \rho_i^{BA} & \rho_i^{BB} \end{pmatrix}$

$$\rho_i^{AA} = \left(1 + \frac{\rho_{i+1}^* l_{i+1}}{\rho_i^* l_i} + \frac{r_i}{\rho_i^* l_i}\right) e^{\frac{d_i}{l_i}}$$

$$\rho_i^{AB} = \left(1 - \frac{\rho_{i+1}^* l_{i+1}}{\rho_i^* l_i} + \frac{r_i}{\rho_i^* l_i}\right) e^{-\frac{d_i}{l_i}}$$

$$\rho_i^{BA} = \left(1 - \frac{\rho_{i+1}^* l_{i+1}}{\rho_i^* l_i} + \frac{r_i}{\rho_i^* l_i}\right) e^{\frac{d_i}{l_i}}$$

$$\rho_i^{BB} = \left(1 + \frac{\rho_{i+1}^* l_{i+1}}{\rho_i^* l_i} - \frac{r_i}{\rho_i^* l_i}\right) e^{-\frac{d_i}{l_i}}$$

and $\hat{J}_i = \begin{pmatrix} \rho_i^{AJ} \\ \rho_i^{BJ} \end{pmatrix}$ with :

$$\rho_i^{BJ} = \frac{1}{2}\left[r_i^*\left(\beta_i - \gamma_i\right) + \rho_{i+1}^* l_{i+1}\left(\beta_{i+1} - \beta_i\right)\right]$$

$$\rho_i^{AJ} = \frac{1}{2}\left[r_i^*\left(\beta_i - \gamma_i\right) - \rho_{i+1}^* l_{i+1}\left(\beta_{i+1} - \beta_i\right)\right]$$

Comparison of NiFe and FeCo free layer : influence of l_{SF}

Free layer :
NiFe/FeCo
or FeCo only

Name	ρ	β	r	γ	Lsf	t
NiCr	140μΩ.cm	0	0.5mΩ.μm²	0.5	20 nm	5 nm
NiFe	25	0.7	0.3	0.7	4.5	
Co50Fe50	16	0.7	0.3	0.7	15	1 t_F
Cu	5	0	0.3	0.7	50	4
Co50Fe50	16	0.7	0.5	0.1	15	3
PtMn	180	0	0.8	0	2	8
NiCr	140	0	0.5	0	20	5

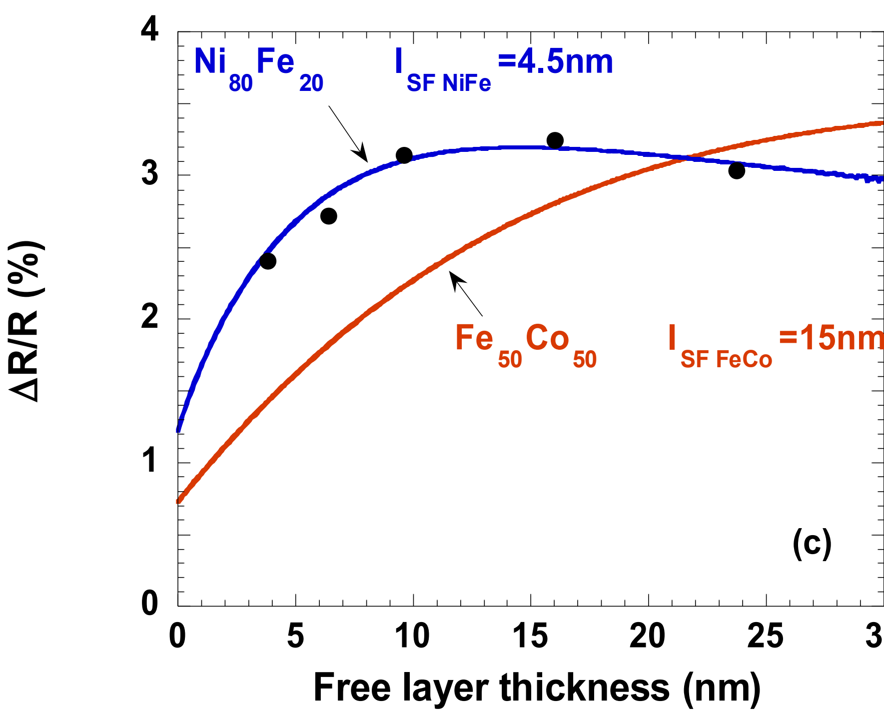

Smooth maximum in CPP GMR versus t_F

Phenomenologically,
$\Delta R\ \alpha\ 1-\exp(-tF/lSF\ F)$
and
$\Delta R/R\ \alpha\ [1-\exp(-tF/lSF\ F]/(tF+cst)$

Data from Headway Technologies

Comparison of Cu and Au spacer layers : influence of l_{SF}

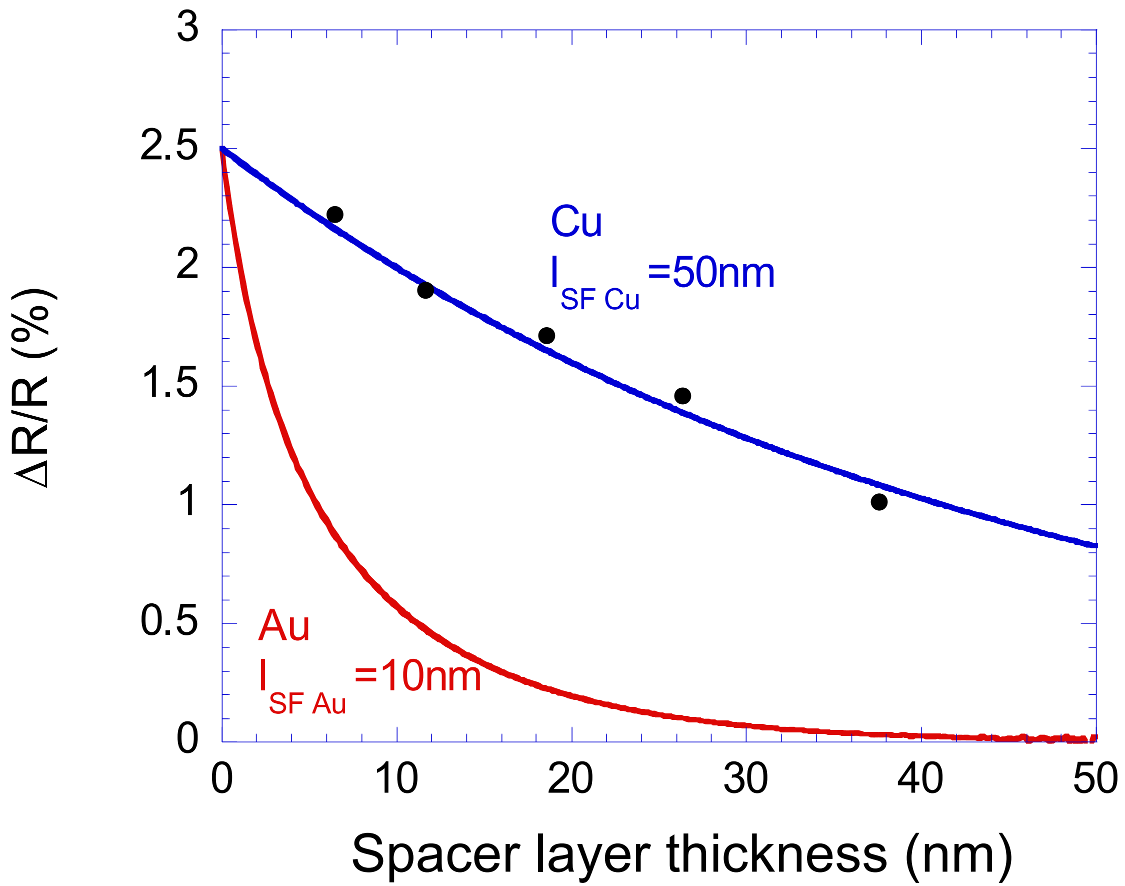

Data from Headway Technologies

Phenomenologically, decrease of ΔR as exp(-tspacer/lSF spacer)
and ΔR/R as exp(-tspacer/lSF spacer)/(tspacer+cst)

Inhomogeneous current distributions in numerous experimental situations…

Current confined paths (CCP) GMR

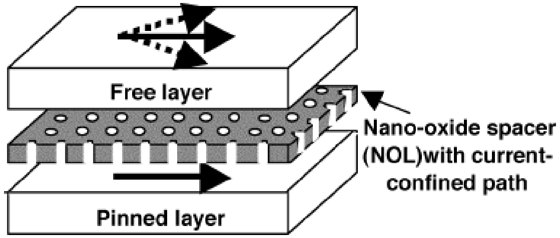

K.Nagasaka et al, JAP89 (2001), 6943
H.Fukazawa et al, IEEE Trans.Mag.40 (2004), 2236

Current crowding effects in low RA MTJ

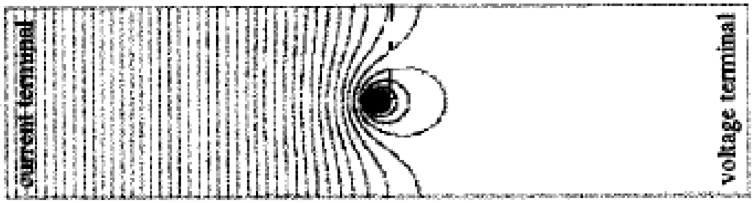

See for instance: J.Chen et al, JAP91(2002), 8783.

Spin transfer oscillators in point-contact geometry

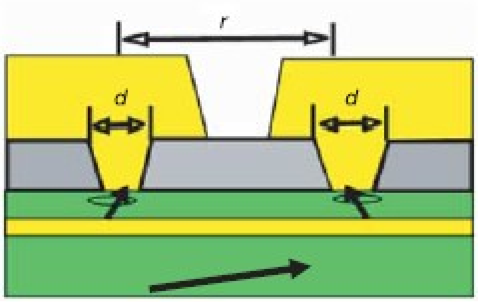

S.Kaka et al, Nat.Lett.437, 389 (2005)
F.B.Mancoff et al, Nat.Lett.437, 393 (2005)

Metallic CPP heads

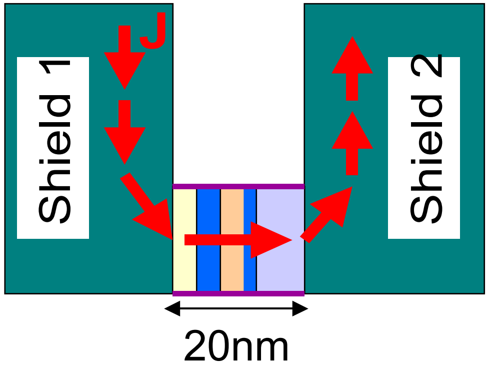

… almost all models of spin-dependent transport assume uniform current

Extending Valet-fert theory at 3D in colinear geometry

$$J_{\uparrow} = \sigma_{\uparrow}\left(-grad\varphi + \frac{1}{e}\frac{\partial \Delta\mu}{\partial z}\right)$$

$$J_{\downarrow} = \sigma_{\downarrow}\left(-grad\varphi - \frac{1}{e}\frac{\partial \Delta\mu}{\partial z}\right)$$

Out-of-equilibrium magnetization

$$\Delta\mu = \frac{m}{\mu_B \nu}$$

energy

DOS

Electrical current:

$$J_{el} = J_{\uparrow} + J_{\downarrow} = -\left(\sigma_{\uparrow} + \sigma_{\downarrow}\right) grad\varphi + \frac{\left(\sigma_{\uparrow} - \sigma_{\downarrow}\right)}{e\mu_B \nu}\frac{\partial m}{\partial z}$$

With $\sigma_{\uparrow} = (1+\beta)\sigma$ $\quad\quad$ $\sigma_{\downarrow} = (1-\beta)\sigma$

$$J_{el} = -2\sigma\, grad\varphi + \frac{2\beta\sigma}{e\mu_B \nu}\frac{\partial m}{\partial z}$$

3D expression of electron current:

$$\vec{J}_e = 2\sigma\,\vec{\nabla}\varphi - \frac{2\beta\sigma}{e\mu_B \nu}\vec{\nabla} m$$

Spin current:

$$J_s = \left(\frac{-1}{e}\right)(J_\uparrow - J_\downarrow) = \left(\frac{-1}{e}\right)\left[-(\sigma_\uparrow - \sigma_\downarrow) grad\varphi + \frac{(\sigma_\uparrow + \sigma_\downarrow)}{e\mu_B \nu}\frac{\partial m}{\partial z}\right]$$

$$J_s = \left(\frac{2\beta\sigma}{e}\right) grad\varphi - \frac{2\sigma}{e^2\mu_B \nu}\frac{\partial m}{\partial z}$$: Spin current

$$J_m = \left(\frac{2\beta\sigma\mu_B}{e}\right) grad\varphi - \frac{2\sigma}{e^2 \nu}\frac{\partial m}{\partial z}$$: Moment current

<u>3D expression of moment current</u>: $$\vec{J}_m = \left(\frac{2\beta\sigma\mu_B}{e}\right)\vec{\nabla}\varphi - \frac{2\sigma}{e^2\nu}\vec{\nabla} m$$

In colinear magnetization J_m is a vector

$$\vec{J}_e = 2\sigma\,\vec{\nabla}\varphi - \frac{2\beta\sigma}{e\mu_B\nu}\vec{\nabla}m$$

$$\vec{J}_m = \left(\frac{2\beta\sigma\mu_B}{e}\right)\vec{\nabla}\varphi - \frac{2\sigma}{e^2\nu}\vec{\nabla}m$$

2 Unknowns: | $\varphi \quad m_z$

Transport equations:

$$\boxed{\begin{aligned} &div\mathbf{J}_{\mathbf{e}} = 0 \\ &div\mathbf{J}_{\mathbf{m}} + \frac{2\sigma}{\nu\, \mathrm{l}_{\mathrm{sf}}^2}\left(1-\beta^2\right)\mathbf{m} = 0 \end{aligned}}$$

Diffusion of charge (with conservation of charge)

Diffusion of spin (without spin conservation due to spin-torque and spin-relaxation

lSF=spin-diffusion length

derived from Valet/Fert: $e\rho_\sigma \dfrac{\partial J_\sigma}{\partial z} = \dfrac{\mu_\sigma - \mu_{-\sigma}}{2l_{SF}^2}$

2 Equations: 1 diffusion of e + 1 diffusion of m

Can be solved in complex geometry with a finite element solver

2D CPP pillar with extended electrodes

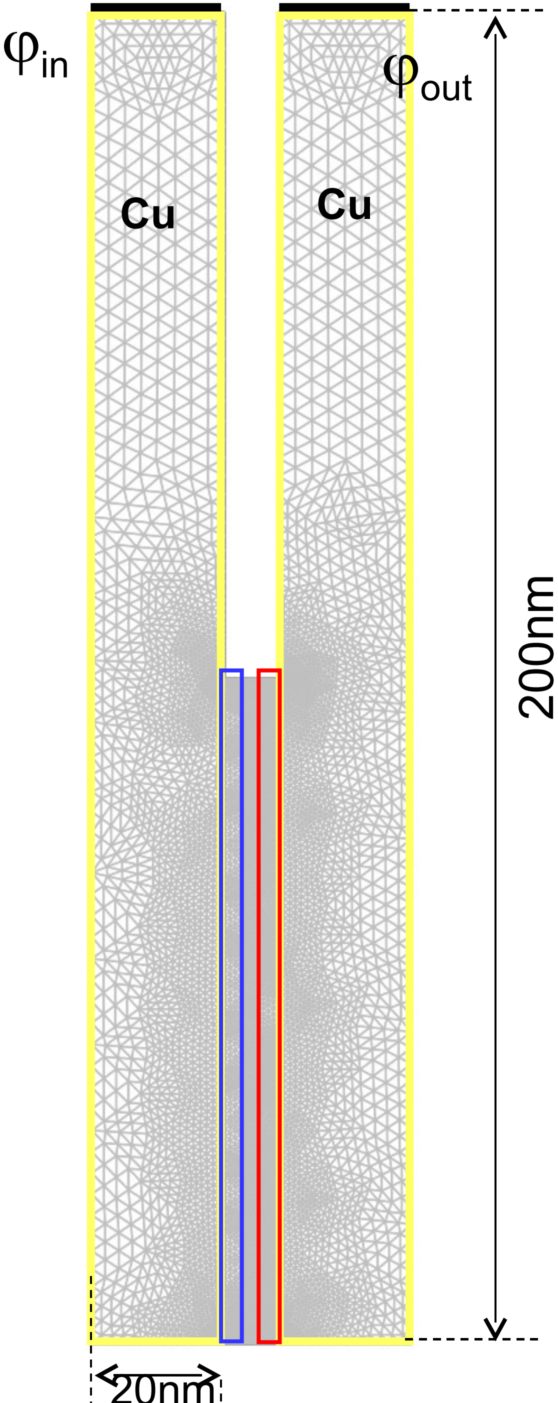

Mapping of charge current

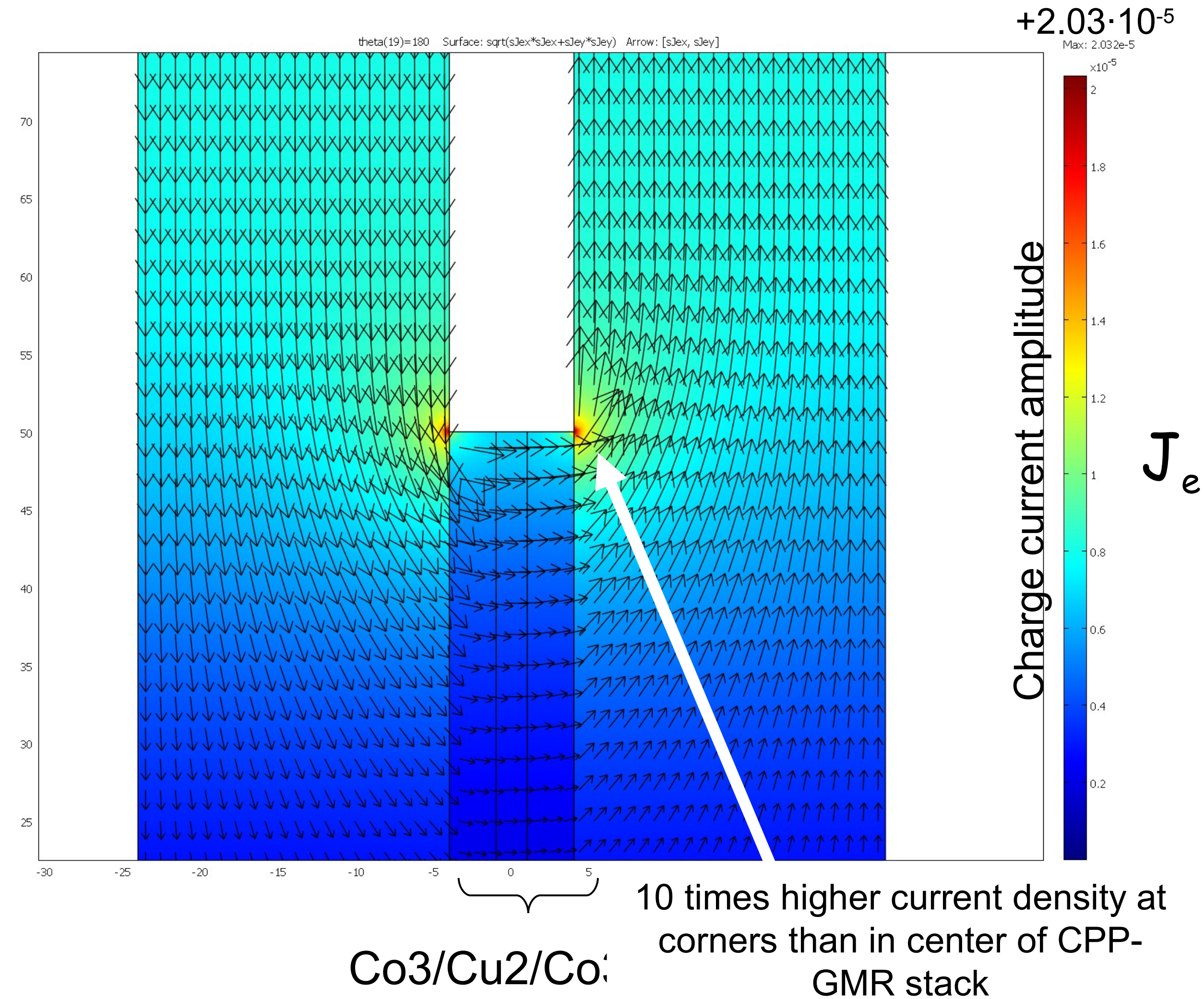

10 times higher current density at corners than in center of CPP-GMR stack

2D CPP pillar with extended electrodes

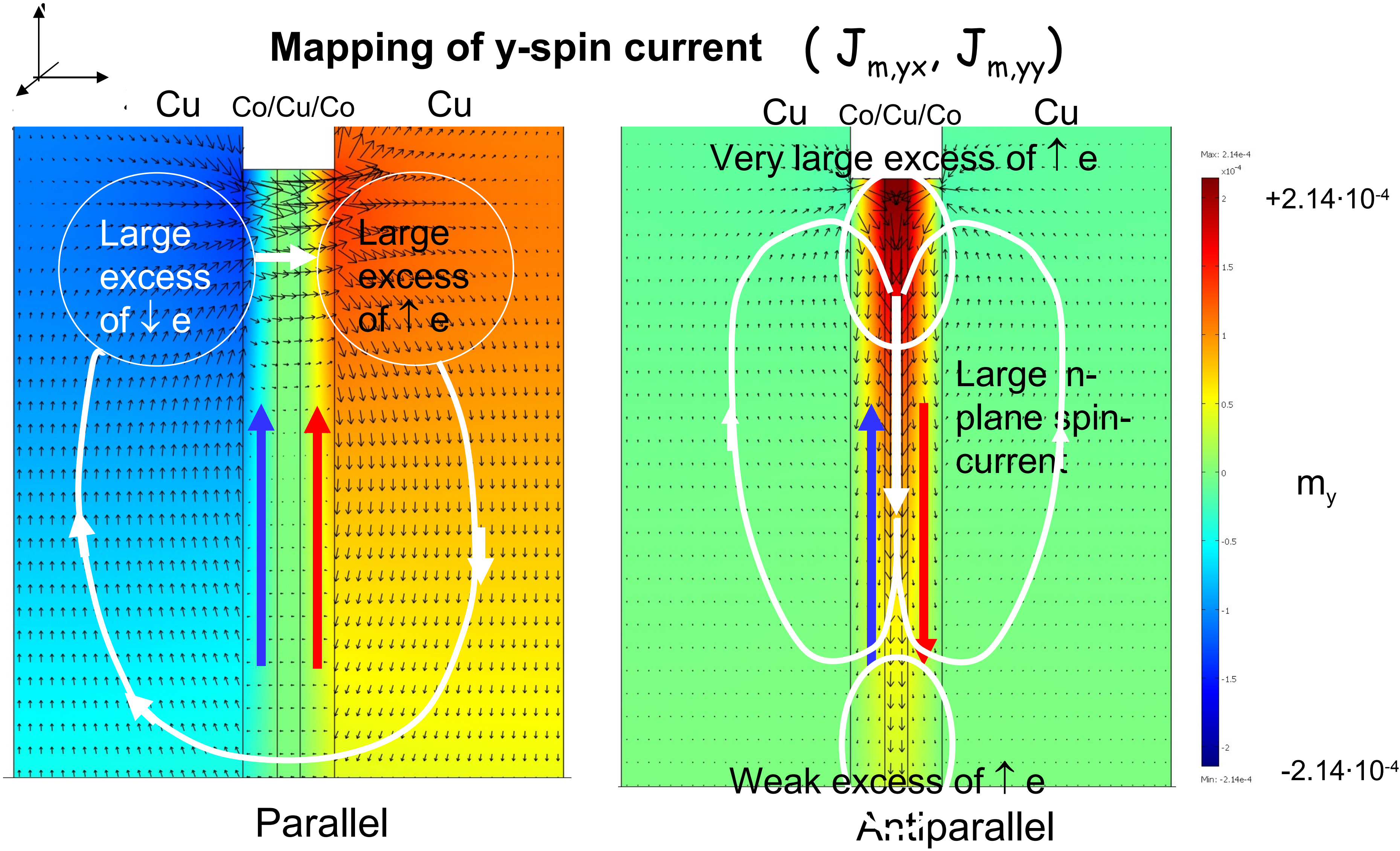

Conclusion on CPP transport

-Serial resistance model can be used at lowest order of approximation to describe CPP transport. However, does not take into account spin-flip.

-With spin-flip, spin accumulation and spin-relaxation play an important role in CPP transport.

-Semi-classical theory of transport describes CPP transport fairly well. CPP macroscopic transport properties (R, $\Delta R/R$) can be calculated from microscopic transport parameters (ρ_σ, l_{SF}, r_σ)

-In complex geometry, charge and spin current can have very different behavior.
Two contributions to j_σ: drift along electrical field and diffusion along gradient of spin accumulation.

Thank you !

Signal/noise ration in CIP MR heads

Signal : $$\Delta V = \Delta R.I$$

Noise : $$V_{Johnson} = \sqrt{4k_B TR\Delta f}$$

Signal/Noise : $$SNR = \frac{\Delta V}{V_{Johnson}} = \left(\frac{\Delta R}{R}\right)\frac{\sqrt{power}}{\sqrt{4k_B T\Delta f}}$$

To maximize the SNR in MR heads, the power dissipated in the head must be as large as possible compatible with reasonable heating and electromigration

$\langle j \rangle \sim 4.10^7 A/cm^2$ used in heads with CIP-GMR~15%